Towards the Development of Thermoresponsive Starch Films

by

Yuhan Huang

A thesis
presented to the University of Waterloo
in fulfilment of the
thesis requirement for the degree of
Master of Science
in
Chemistry (Nanotechnology)

Waterloo, Ontario, Canada, 2018

Author's Declaration

I hereby declare that I am the sole author of this thesis. This is a true copy of the thesis, including any required final revisions, as accepted by my examiners.

I understand that my thesis may be made electronically available to the public.

Abstract

Wound dressings are an important part of the global wound care market. In addition to having desirable physical properties such as flexibility and gas permeability, it is also important that they be easily removed. As wound dressings tend to stick to wounds due to the reduction of exudate, the removal of the dressing can be painful and cause secondary injuries. This issue can be minimized by using thermoresponsive (TR) materials. At body temperature, TR dressings are designed to be hydrophobic and adhere strongly to a wound, but upon cooling below body temperature they become hydrophilic and adhere less strongly thus allowing for easy removal of the dressing without causing damage to the wound.

The TR films/membranes that have been examined for TR wound dressings are derived from synthetic polymers. Synthetic polymers can have environmental and health concerns when it comes to medical applications. An alternative to using TR synthetic polymers is TR biopolymers which have the advantages of low-cost and biocompatibility. TR hydroxybutylated starch nanoparticles (HBSNPs) have been developed in the Taylor group. The objective of this work is to develop TR hydroxybutyl starch-based films with mechanical properties that are favorable for wound dressing applications.

Films prepared from HBSNPs and using glycerol (GY) as plasticizer lacked stability in that they tended to become brittle even when stored in an environment with controlled humidity. Different approaches to improving their stability were examined. Sorbitol or mixtures of sorbitol and GY were examined as plasticizers but the resulting films still readily cracked and were opaque. Blending the HBSNPs with different amounts of poly (vinyl alcohol) (PVA) and GY generally did not produce stable films unless the amount of GY and PVA was very high (40 wt.% compared to the SNPs). The mechanical properties of the more stable HBSNP/PVA/GY films were determined

by dynamic mechanical thermal analysis (DMTA) via tensile testings. Under 50 % RH, films with higher PVA had greater tensile strength and could be extended longer. No thermal transitions of these films or of the HBSNPs themselves were detected by differential scanning calorimetry (DSC). mPEG-grafted HBSNPs were developed in order to prepare a stable and thermoresponsive film. However, this approach was ultimately abandoned as the mPEG-grafted HBSNPs were difficult to purify and the starting material was expensive. Hydroxybutylated corn starch (HBCS) films reinforced with unmodified SNPs were prepared. Incorporation of the SNPs enhanced the physical properties of the HBCS films. Attempts to determine their thermoresponsivity by measuring their water contact angles were unsuccessful as the films were not stable to water. It was concluded that crosslinking of the HBCS films would be necessary to provide the needed water stability for contact angle measurements. Gels were obtained when using hexamethylene diisocyanate (HMDI) to crosslink the HBSNPs. The gels appeared to be thermoresponsive as determined by DSC; however, the results were difficult to reproduce possibly due to different crosslink densities within the gels. HBCS films crosslinked with glyoxal (GX) or oxidized sucrose (OS) were also prepared. Although the GX and OS crosslinks appeared to increase the stability of the HBCS films in water, they were still not highly stable.

Acknowledgements

First, I would like to express my gratitude to my supervisor, Prof. Scott. D. Taylor for his guidance and support. It is such a challenging project that I cannot get here without his encouragement and knowledge. I would like to thank my co-supervisor, Prof. Leonardo Simon, who provided useful suggestions and gave me strength to carry on when I was lost and lacked ideas. I would like to thank my committee members, Prof. Juewen Liu and Prof. Jean Duhamel for their support, Prof. Marios loannidis for allowing me to use the video contact angle system and Ralph Dickhout for the training on DSC. I would like to thank the members of the EcoWin collaboration and the members of the Taylor group for their generous help and company. Last but not the least, I would like to thank my dear families for their great selfless support which makes me stronger than I was ever before. I am also very grateful to my boyfriend for his company and encouragement during many stressful moments.

Table of Content

List of Figures

List of Tables

List of Schemes

List of Abbreviations

- AgNPs Sliver Nanoparticles
- AIBN Azobisisobutyronitrile
- BDA 1,4-butanediamine
- BE_mS 3-[2-Butoxy(ethoxy)$_m$]-2-Hydroxypropyl Starch Ether
- CMC Carboxymethylcellulose
- CI Cadexomer Iodine
- Dh Hydrodynamic Diameter
- DLS Dynamic Light Scattering
- DMAC Dimethyl Acetamide
- DMAP 4-Dimethylaminopyridine
- DMTA Dynamic Mechanical Thermal Analysis
- DMSO Dimethyl sulfoxide
- DSC Differential Scanning Calorimetry
- DW Deionized Water
- EDC 1-Ethyl-3-(3-dimethylaminopropyl) carbodiimide
- EDX Energy-Dispersive X-Ray Spectroscopy
- FTIR Fourier-transform Infrared Spectroscopy
- GX Glyoxal
- GY Glycerol
- HBCS Hydroxybutylated Corn Starch
- HBPS 2-Hydroxy-3-Butoxypropyl Starch
- HBSNP Hydroxybutylated Starch Nanoparticles

- HCl Hydrochloric Acid
- HIPS 2-Hydroxy-3-Isopropoxypropyl Starch
- HMDI Hexmethylene Diisocyanate
- IPN Interpenetrating Polymer Network
- LCST Lower Critical Solution Temperature
- LDI Lysine Methyl Ether Diisocyanate
- MALDI-TOF Matrix Assisted Laser Desorption Time of Flight
- MBAm Methylenebisacrylamide
- Mn Number average molecular weight
- mPEG Methoxypolyethylene glycol
- MR Molar Ratio
- MS Molar Substitution
- MW Molecular Weight
- MTT 3-(4,5-Dimethylthiazol-2-yl)-2,5-Diphenyltetrazolium Bromide
- NMR Nuclear Magnetic Resonance
- PBS Phosphate Buffered Saline
- PCL Polycaprolatone
- PEO-PPO-PEO Poly(Ethylene Oxide)-Poly(Propylene Oxide)-Poly(Ethylene Oxide)
- PEG Polyethylene glycol
- PETMP Pentaerythritol Tetra
- PNIPAAM Poly (*N*-Isopropylacrylamide)
- PVA Polyvinyl Alcohol
- RE Reaction Efficiency

- R_h Hydrodynamic Radius
- RH Relative Humidity
- rt room temperature
- Semi-IPNs Semi-Interpenetrating Networks
- SMPs Starch-Maleate-Polyvinyl Alcohol hydrogels
- SNPs Starch Nanoparticles
- SPUU Segmented Polyurethane Urea
- TAS Tertiary Amine Starch Ether
- T_c Cloud Point Temperature
- Tg Glass transition temperature
- TEM Transmission Electron Microscopy
- TGA Thermogravimetric Analysis
- TR Thermoresponsive
- TRPs Thermoresponsive Polymers
- TRPU Thermoplastic Polyurethane
- TRWDs Thermoresponsive Wound Dressings
- UCST Upper Critical Solution Temperature
- WVTR Water Vapor Transfer Rate

Chapter 1 Introduction

1.1 Introduction to Thermoresponsive Wound Dressing

Applying wound dressing is necessary for the acceleration of wound healing as the exposure of wounds to the external environment may cause problems like infections and dehydration. One important part of the pharmaceutical wound care global market is wound dressing. The main goal of wound care is to heal the wound rapidly with decent functional and cosmetics outcomes since the human body alone cannot heal dermal damage completely. The functions of wound dressings should include creating a moist environment, absorbing body fluids, providing protection from secondary infections, and allowing for sufficient gas exchange.[1] However, it is known that the removal of wound dressings can be quite painful. It is attributed to the reduction of the exudate, which increases the adherence of the dressing to the wound bed. Thermoresponsive wound dressings (TRWDs) are being introduced to deal with this issue. They adhere strongly to the wound at body temperature, but upon cooling, their adhesive properties decrease significantly thus allowing for easy removal of the dressing without causing damage to the wound. This can avoid the high risk of secondary infection and make the removal of the wound dressing more bearable.[2]

1.2 Wound Dressings

Wound dressings are made from both natural and synthetic material. Traditional gauze dressings are made of woven and nonwoven fibers of cotton and rayon polyester. The removal can be extremely painful as these materials are usually dehydrated due to moisture evaporation. Hydrogels, hydrocolloids, foams and biological materials are categorized as modern dressing

materials. Hydrogel wound dressings are obtained from swellable hydrophilic materials such as poly(methacrylates) and polyvinylpyrrolidine. They can rehydrate the wound with significant amounts of water. As a result, less exudate will be absorbed. They maintain a moist environment due to their porous structure and provide thermal insulation. Hydrocolloids are made from gel forming agents such as carboxymethylcellulose (CMC), gelatin and pectin. They are quite useful because they can adhere to both dry and moist sites. However, the occlusive outer cover of the hydrocolloid can prevent water vapour exchange with the surroundings, which in turn may inhibit gas permeability, delaying the healing process. The foam dressings are generally prepared using polyurethane foam or polyurethane foam films. Biological dressings are usually derived from materials such as starch, chitosan, collagen.[1]

1.3 Properties of Wound Dressings

There are some basic properties that all wound dressings should possess. These properties are discussed below.

1.3.1 Mechanical Property

Wound dressing materials are required to be durable, flexible, and elastic so that they can handle stress from different body parts, such as the elbow. Mechanical properties are usually determined from the strain at break, tensile strength, and elastic modulus. To determine these properties, films are cut into dumbbell shaped strips which are deformed in a tensile test experiment. During this process, the tension load (stress) is monitored as a function of elongation (strain) to yield a stress-strain plot. Interpretation of the stress-strain plot provides information about the mechanical properties of the tested material. A typical stress-strain curve is shown in **Figure1.1**. The slope of the linear portion, labeled as ‘A’, gives the elastic modulus, reflecting the

resistance to an elastic deformation. C is the point at which a film breaks and is related to the elastic limit. B is the strain at break. It is equal to $l/l_0 - 1$where l_0 and l are the length of the original and elongated dumb-bell, respectively. The T point corresponds to the tensile strength of the material, the maximum strength that the material can handle at break.[1]

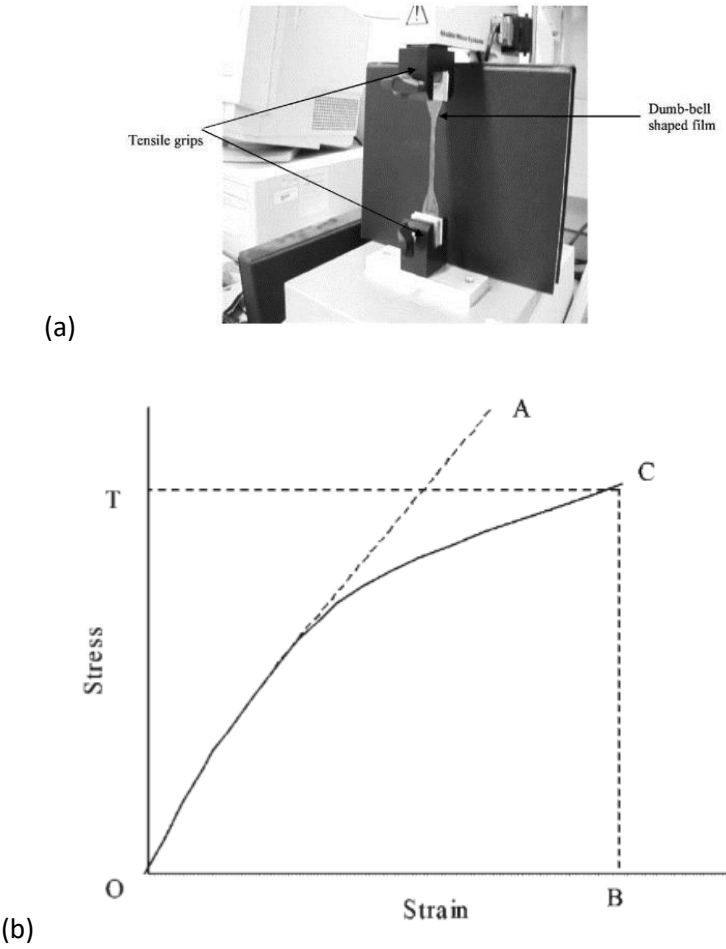

Figure 1.1. (a) A dumb-bell shaped film being stretched between two grips in the tensile mode (b) A typical stress-strain curve.[1]

The viscoelastic properties of the films can be evaluated via dynamic mechanical thermal analysis (DMTA) as a sinusoidal stress and heat are applied simultaneously. The variation of storage modulus (E'), loss modulus (E"), and loss tangent (tan δ) as a function of temperature can be graphed.

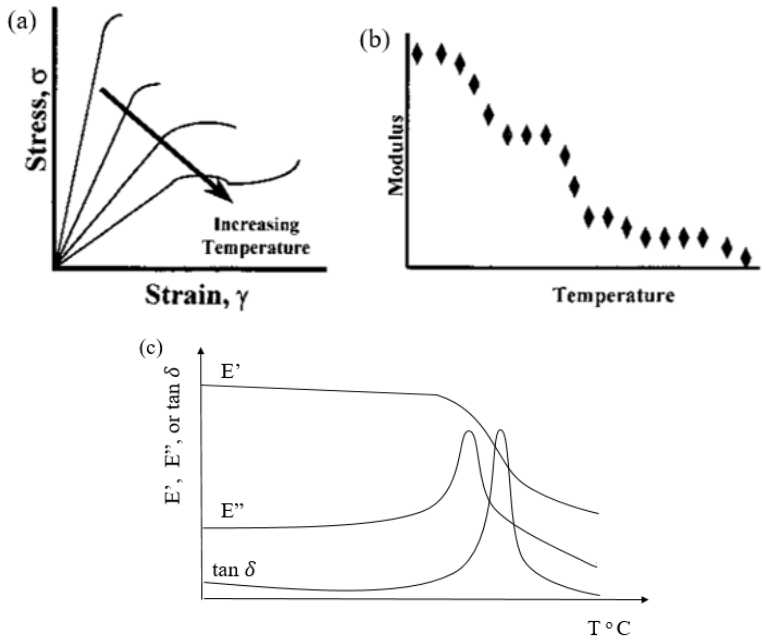

Figure 1.2. (a)Plots of typical stress-strain curves with increasing temperature. (b) Plot of modulus as a function of temperature. (c)Plots of storage modulus (E'), loss modulus (E") and loss tangent (tan δ) as a function of temperature.[3]

The initial linear slope of the stress-strain curve in **Fig 1.2A** is defined as the modulus. As the temperature increases, the modulus of the material decreases as the material becomes more ductile. The elastic response of the material is measured by the storage modulus E', representing the energy stored during deformation while the viscous response is measured by the loss modulus E", indicating the energy dissipated as heat. This can be compared to a bouncing ball. After it has hit the ground, E' is related to how high it will bounce back while E" represents the energy lost as heat. Tan δ is defined as the ratio of the loss modulus over the storage modulus. A decreasing tan δ value indicates that the material becomes more elastic.[3]

1.3.2 Fluid Uptaking and Swelling

The capability of absorbing exudate is an important property of wound dressing materials. To determine this, dressing materials of known weight (W_d) are immersed in phosphate-buffered saline (PBS) solution, pH 7.4, for a given period of time. For film materials, excess fluid is removed by blotting the film between filter papers. The sample is weighed immediately after blotting. Water content is calculated as $(W_t-W_d)/W_d$. where W_t is the weight after immersion and blotting.[4]

Water vapor transmission rate (WVTR) is usually determined by measuring the amount of water lost to the atmosphere over a certain period of time. Gravimetric techniques are utilized to test the weight loss due to water vapor loss. During the testing, the sample is placed in a cup containing 20 mL of test solution. The cup will be placed on a pan balance, which is connected to an electronic data capture device to record the weight loss.[1]

1.3.3 Biocompatibility

The wound dressing must be biocompatible (non-toxic). Biocompatibility studies are conducted by directly exposing cells (in tissue culture) to dressing materials or the leachates extracted from them. Cell viability is usually detected using a yellow tetrazole dye (MTT) assay. In living cells, MTT is reduced by an NAD(P)H-dependent cellular oxidoreductase to form purple formazan. The purple formazan dissolves in dimethyl sulfoxide. The solution color is detected with a spectrophotometer. Cells undergoing rapid division display a high rate of MTT reduction.[2]

1.4 Introduction to Thermoresponsive Polymers

TRWDs are based on thermoresponsive polymers (TRPs). There are two main categories of TRPs. TRPs with lower critical solution temperatures (LCST) and ones with upper critical

solution temperatures (UCST) (**Fig 1.3**). TRPs with an LCST appear to be clear and soluble below their LCST (often called the cloud point, T_c) and turn turbid above the LCST. In contrast, TRPs exhibiting a UCST demonstrate the opposite solubility behaviour with temperature.[5] For TRWD applications, the TRPs with LCSTs are utilized.[1,4]

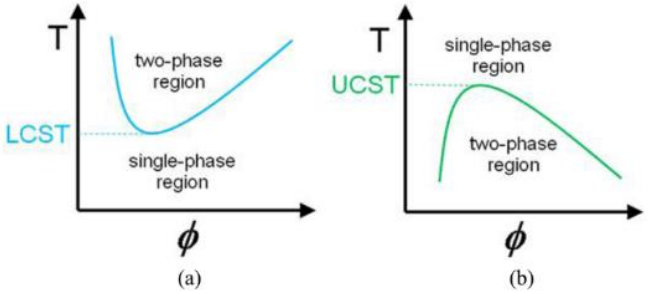

Figure 1.3. Phase diagrams (temperature (T) vs. polymer volume fraction (ϕ)) for TRPs in solution. (a) Phase diagram for TRPs having a lower critical solution temperature (LCST). (b) Phase diagram for TRPs having an upper critical solution temperature (UCST).[5]

For TRPs exhibiting an LCST, the polymer stays solvated below the LCST due to hydrogen bonding between the hydrophilic regions of the polymer and water molecules. The hydrophobic regions of the polymer are surrounded by a clathrate which is an ordered arrangement of water molecules. Although the H-bonded and ordered water molecules contribute to a decrease in entropy, the free energy of the system remains negative (energetically favorable for a homogenous solution) as the presence of a vast number of polymer-water hydrogen bonds results in a large negative enthalpy. Considering Gibbs equation, $\Delta G = \Delta H - T\Delta S$ (where G is the Gibbs free energy, H is the enthalpy and S is the entropy), the ΔH term is the main contributor to the overall negative ΔG term of the system. When the temperature increases above the LCST, the enthalpy of the system becomes less negative as a result of disruption or weakening of the polymer-water hydrogen bonds. The dissociation of water molecules from the polymer increases the entropy of the system. The entropy component dominates the contribution to the negative free energy of the system, and becomes the main driving force for the phase separation above the LCST.

LCST-type TRPs can exhibit two distinctive phase transition behaviors: a coil-to-globule transition (intramolecular aggregation) and/or intermolecular aggregation. A coil-to-globule transition describes a process by which a linear flexible polymer chain adopts other thermodynamically stable conformations due to a change in temperature. Below its LCST, a TRP completely dispersed in water adopts a random coil conformation via the formation of extensive hydrogen bonding between the polymer and water molecules. Above the LCST, polymer-water hydrogen bonding is disrupted which results in intramolecular aggregation (the polymer collapses into a globular conformation). One example of such a TRP is poly(*N*-isopropylacrylamide) (pNIPAAM) which has an LCST of 32 ºC in water.[6] The coil-to-globule transition of pNIPAAM, is supported by the fact that the hydrodynamic radius (R_h) below the LCST decreases as the temperature increases (**Fig.1.4**).[7]

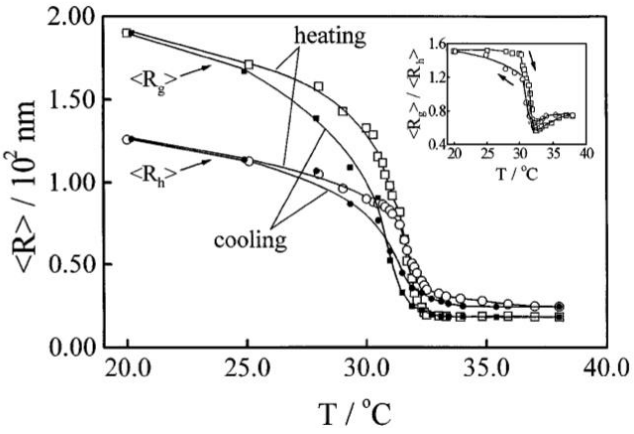

Figure 1.4. Temperature dependence of the average radius of gyration [R_g] and the average hydrodynamic radius [R_h] of pNIPAAM, respectively, in the coil-to-globule (heating) and the globule to-coil (cooling) processes.[7]

TRPs that exhibit a phase transition involving intermolecular aggregation, but without experiencing the coil-to-globule transition, are usually amphiphilic block copolymers that consist of hydrophilic and hydrophobic regions. Below the LCST, the polymer chains are typically in a random coil conformation in an aqueous dispersion. As the critical temperature is reached the coil

conformation is no longer thermodynamically stable, which results in intermolecular association of the polymer chains into large aggregates.

1.5 Measuring Thermoresponsivity in Membranes and Films

TRWDs are produced as films or membranes. One method of determining the LCST of TR membranes or films is to detect the change in heat flow using differential scanning calorimetry (DSC). As the polymer undergoes a thermal transition, it requires more heat which is shown as an endothermic peak in the heat diagram (**Fig 1.5**). This peak indicates the collapse of the polymer in the hydrated state while no variation is observed for the dehydrated state. The down-up trend suggests a phase transition has occurred and the lowest point in the curve is the LCST.[2]

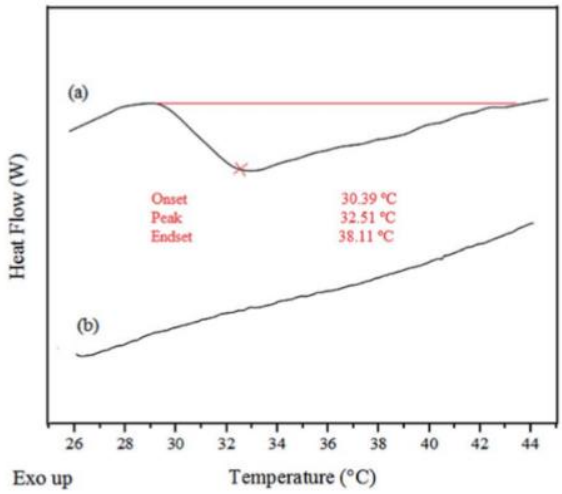

Figure 1.5. Thermogram of polyurethane-poly(*N*-isopropylacrylamide) membrane in a) a hydrated state, b) a dehydrated state.[2]

A TR film will have different bulk and surface hydrophilicity above and below its LCST. Hence, the amount of water absorbed and the water contact angle of the TR film can be used to characterize the thermoresponsivity of the film.[2] As the temperature of the TR film approaches the LCST, the material becomes more hydrophobic and the water contact angle increases. Normally, the optimum water contact angle for cell adhesion and proliferation is 60-70°.[2]

1.6 Examples of Thermoresponsive Wound Dressings

Whether it is traditional or modern wound dressing, secondary injury may occur when the separation is not performed carefully. TRPs have been exploited as one of the solutions for this problem. PNIPAAM films have been examined as a TRWD. Since the body temperature (37 ºC) is higher than the LCST of pNIPAAM (32 ºC), the material will remain hydrophobic above the LCST and adhere to the wound. The removal of the dressing is easily achieved by lowering the temperature below the LCST. Nevertheless, it is found that pNIPAAM has the disadvantage of poor flexibility in both dry and hydrated states.[6] To improve pNIPAAM's wound dressing properties it is often combined with other polymers. Some examples of this are discussed below.

In 2008, Reddy et al. examined semi-interpenetrating polymer networks (semi-IPNs) consisting of segments of polyurethane urea (SPUU) and pNIPAAM as a material for TRWDs. The material was prepared by radical polymerization of pNIPAAM with varying amounts of methylenebisacrylamide (MBAm) crosslinker in the presence of SPUU (**Scheme 1.1**) in dimethyl acetamide (DMAC) at 80 °C under vacuum over 6 h. This yielded films of semi-IPNs. The SPUU and pNIPAAM were physically entangled with each other, which means that only breaking chemical bonds could separate them. Films with differing compositions were obtained that possessed good mechanical properties for TRWDs in both the dry and hydrated states. In addition, NIH3T3 fibroblasts attached and detached from the films with varying temperature (best detachment occurred at 15 ºC). Moreover, these film extracts did not show significant cytotoxicity.[6]

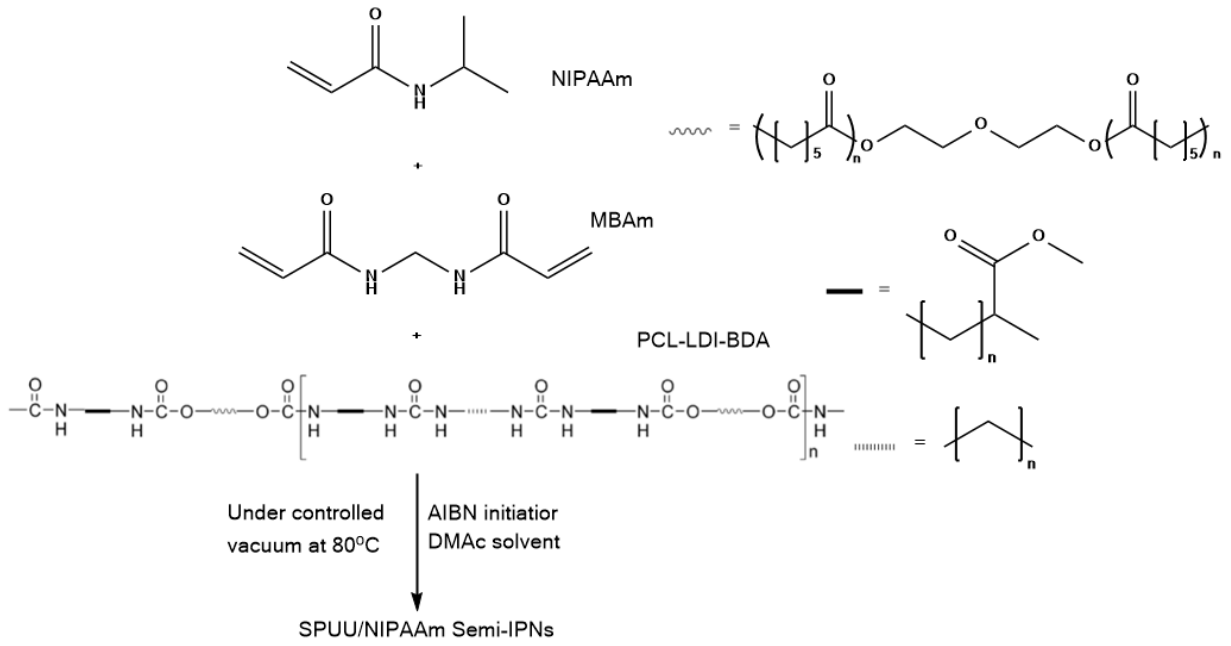

Scheme 1.1. Synthesis of semi-IPNs by Reddy et al.[6]

A chitosan-based hydrogel was shown to have potential as a TRWD by C. Radhakumary et al.[4] An aqueous solution of thiolated chitosan was reacted with NIPAAM monomer in the presence of AIBN at 60 ^{o}C for 3 h. The contents were poured into a disposable polystyrene mould and cured at 45–50 ^{o}C for 48 h, which gave the resulting chitosan hydrogel as a film (**Scheme 1.2**). The LCST of the film, as determined by DSC, was 30.4 ^{o}C. The water contact angle decreased from 113 degrees to 47 degrees as the temperature descends below the LCST, indicating that the material became more hydrophilic below its LCST. The film exhibited cytocompatibility, adequate mechanical strength and was removable from tissue culture templates by lowering the temperature below the LCST.

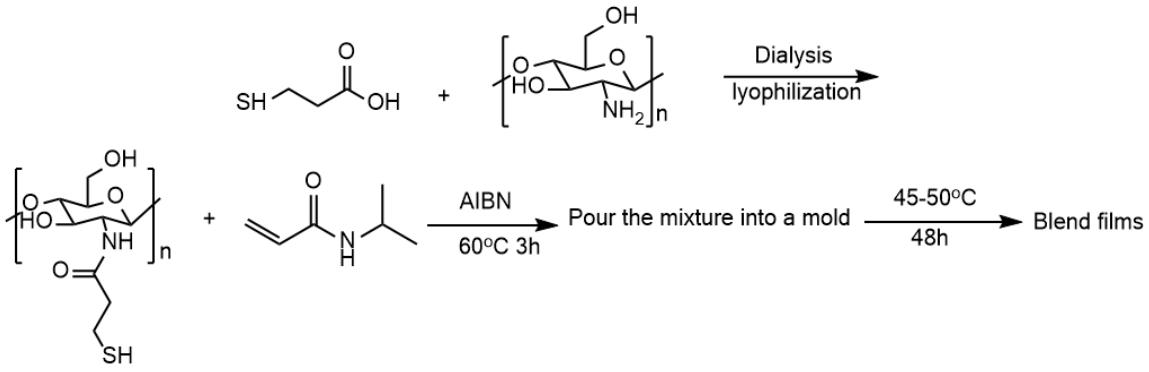

Scheme 1.2. Synthesis of a TR chitosan hydrogel by C. Radhakumary et al[4]

Very recently, Abdali et al. investigated in detail semi-IPNs made up of a thermoplastic polyurethane (TRPU) elastomer and crosslinked pNIPAAM embedded with silver nanoparticles (AgNPs) as antibacterial TRWDs. The material was prepared by a thiol-ene reaction by reacting TRPU with varying amounts of pNIPAAM, *N*,*N*-methylenebisacrylamide (MBA), pentaerythritol tetra (3-mercaptopropionate) (PETMP) in dimethylacetamide (DMAC) and using azobisisobutyronitrile (AIBN) as a free radical initiator in the presence or absence of silver nitrate (**Scheme 1.3**). When the reaction was performed in the presence of silver nitrate, the single electron provided by the initiator, reducing the silver ions to metallic silver, which resulted in silver nanoparticles, a known antibacterial, becoming embedded into the polymer network. The reaction was performed in a Teflon mould at 90 ^{o}C for 12 h which yielded the desired semi-IPNs as membranes.[2]

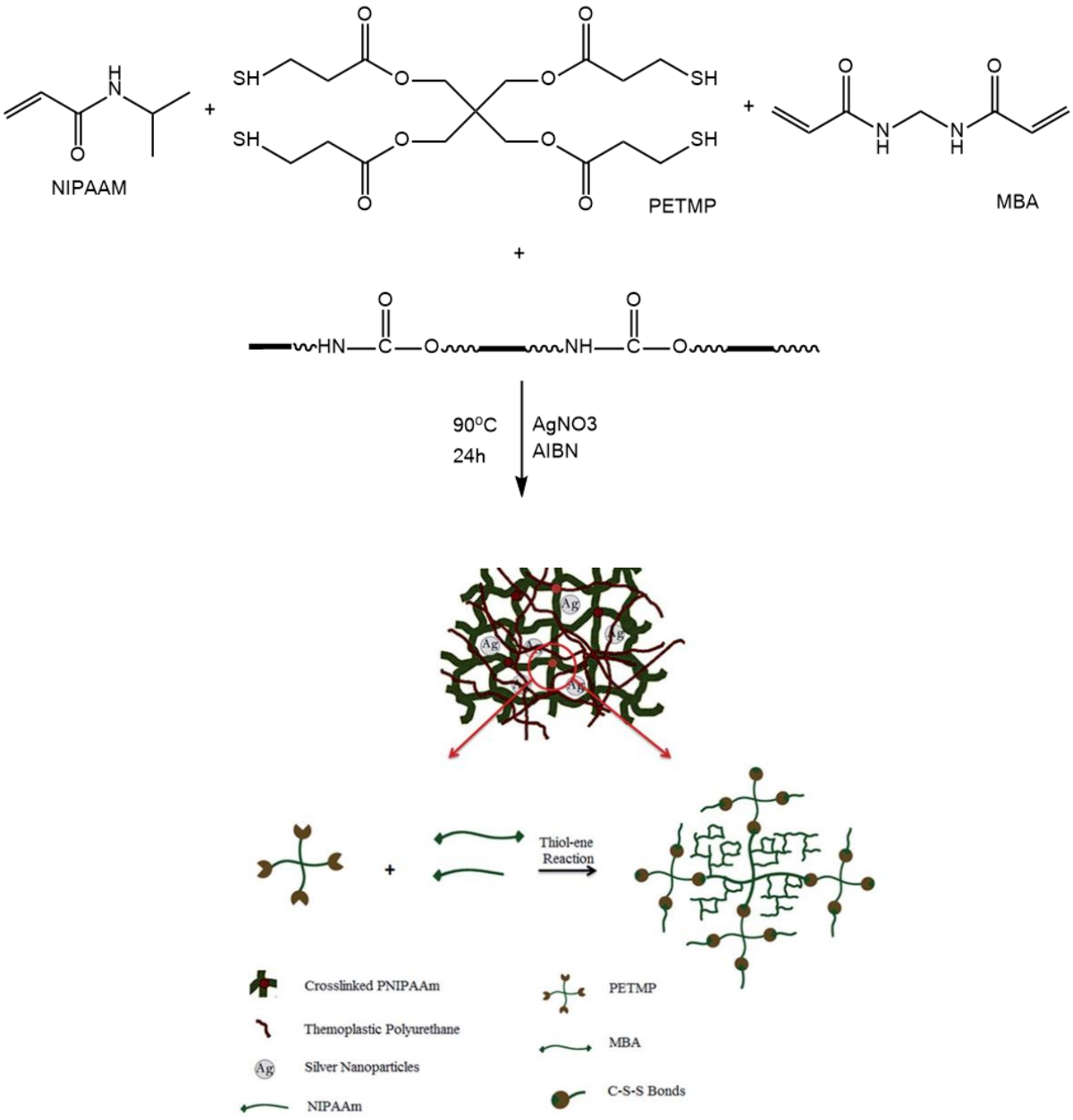

Scheme 1.3. Synthesis of the membranous TR wound dressings by Abdali et al[2]

It was found that the presence of the $AgNO_3$ decreased the density of polymerization. The silver ions competed with the pNIPAAM and MBA monomers for the reaction with the free radicals generated from the initiator. Eventually, this phenomenon led to networks with lower crosslink density.

The thermoresponsivity of the hydrated membranes was determined via DSC and by measuring water contact angles at different temperatures. The LCSTs of the hydrated membranes were around 32.5 ^{o}C which is close to the LCST of pure pNIPAAM hydrogel.

The amount of stratum corneum removed from the surface of the skin by the dressing membranes was assessed at two different temperatures (below and above LCST). There was a significant difference in the percentage of desquamated area at the two studied temperatures with a lower percentage of desquamated area removed from the skin after cooling below the LCST. This result showed appropriate function of the prepared dressings for easy peeling.

Other important characteristics of wound dressings is the ability to preserve wounds from external pressure and mechanical shocks. Therefore, wound dressings must be elastic and unlikely to rip. In addition, strength and flexibility must be maintained during the healing period. The tensile properties (tensile strength, modulus, and elongation at break) of the membranes were evaluated from their stress–strain curves. Very good flexibility of the membranes not containing AgNPs (300 to 650% elongation at break) was preserved when they were in their fully hydrated state.

An ideal dressing should control evaporative water loss at an optimal rate from the wound bed to prevent scab formation due to excessive dehydration and desiccation of wounds. However, accumulation of exudates can cause wound maceration and damage surrounding tissues; therefore, the dressings should absorb these extra exudates and have absorptive properties. Abdali et al found that the average values of water vapour transmission rates (WVTR), water vapour permeability, and water vapour permeance of their membranes were comparable to the commercial products suitable for low to moderated exuding wounds.

A continuous supply of oxygen to the tissue is vital for the healing process and resistance to infection. Oxygen permeation through membranes was evaluated and found was found that the membranes with the highest pNIPAAM and AgNP content were formed to display better performance for transmitting oxygen. This was attributed to the lower crosslink density of these samples.

Dispersion of the AgNPs into the membrane matrix, as well as the size of these particles were elucidated by EDX and TEM. The presence of well-dispersed AgNPs with an average size around 30-50 nm was found. The membranes, with and without AgNPs, were found to be biocompatible based upon an MTT assay against human dermal fibroblast cells. Finally, the antimicrobial activity of the AgNP membranes was demonstrated against *P. aeruginosa*, *S. aureus*, and *C. albicans* bacterial. The cell viability of semi-IPNs containing AgNPs detected by MTT rays showed no significant difference compared with the semi-IPNs without AgNPs.[2]

1.7 Starch

As many TR synthetic polymers are not biocompatible or expensive to prepare, researchers have begun examining less expensive bio-based substances as base materials for preparing TRPs. One such biomaterial is starch. Starch plays a major role in energy storage for many plants. It is made up of two major components: amylose and amylopectin. Amylose is basically a linear α-l,4-linked-D-glucan while amylopectin is a branched polysaccharide with α-1,4-linked D-anhydroglucose chains and α-1,6-linked branches (**Fig. 1.6**). Generally, starch molecules arrange themselves in semi-crystalline granules.[8]

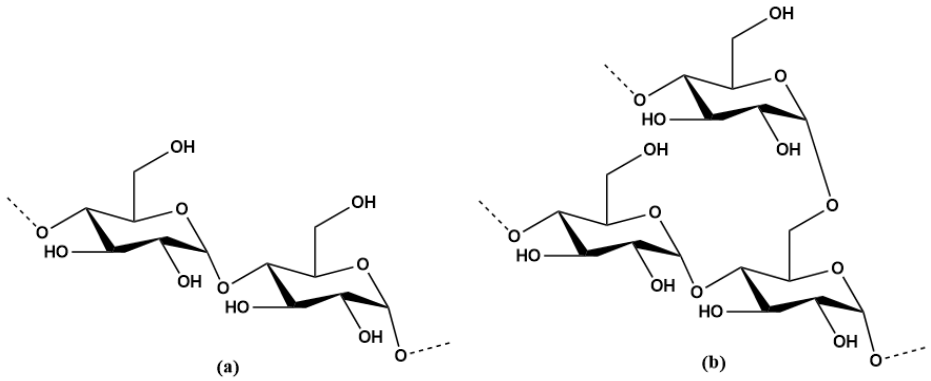

Figure 1.6. Chemical structure of (a) amylose and, (b) amylopectin

1.8 Starch-based Films

There are a number of methods for preparing starch films. One method is by dispersion casting. After gelatinization and homogenization, aqueous starch dispersions are cast on non-adhesive substrates (i.e. silicone) and dried under controlled conditions. However, native starch films are quite brittle compared to many synthetic polymer films. To increase the flexibility and durability of the starch films, a plasticizer is usually employed. Commonly used plasticizers are glycerol, sorbitol and other polyols. These plasticizers help space the starch chains apart, thus decreasing their crystallinity.[9]

Thermoplastic starch films can be made by thermal processing. As starch becomes soft at high temperature (below the degradation temperature), it can be molded into a film. This can be done in an extruder where the starch is drawn through a die of the desired cross section at high temperature and under high sheer in the presence of a plasticizer.[6] It can also be compression molded in a hot press.[8]

Starch films, in the form of a fiber, can also be made via electrospinning. Electrospinning is a method of producing fibers using electric force. When very high voltage is applied to liquid

droplets containing a polymer, the droplets become charged and the droplets stretch due to electrostatic repulsion. Eventually, a stream of the liquid erupts from the surface. The solvent evaporates from the jet stream in flight, and the polymer fiber is deposited on a grounded surface. This process usually produces films of high porosity. Finding an appropriate solvent remains a critical issue for starch electrospinning. Starch aqueous dispersions do not work very well while DMSO or DMSO/water mixtures do not dry well during the process. Other polymers, such as polycaprolactone, poly(vinyl alcohol), poly(lactic acid) can be added. However, in these cases, the starch is used as a filler, rather than being the main fiber material.[10,11]

There are several factors that affect starch films. One of them is amylose-amylopetin content. Films with higher amylose content would exhibit higher degree of crystallinity while higher amylopectin content would have more amorphous domains. In terms of mechanical and thermal properties, films containing more amylose show higher modulus, tensile strength and glass transition temperature.[12,13]

The type of plasticizer can affect the properties of the film. Plasticizers disturb the hydrogen bonding along the polymer chains. The most commonly used plasticizer is glycerol as it is a relatively low molecular weight compound that can penetrate the starch film matrix more effectively than larger polyols. Generally, the starch (often 3 % starch to water by weight) is dispersed at elevated temperatures followed by the addition of glycerol (30 % glycerol to starch by weight) and the mixture is then cast resulting in a film. Moisture in the films also acts as a plasticizer.

Starch films are often incapable of maintaining their integrity and become brittle due to plasticizer migration and water loss. Consequently, they are usually stored in an environmental chamber with controllable humidity or in a desiccator loaded with saturated salt solution.[9,14]

Park et al prepared starch/PVA blended films plasticized with glycerol, sorbitol and citric acid.[14] It was found that as the amount of plasticizer increased, the starch films became more ductile in terms of lower tensile strength (**Fig. 1.7a**) and higher elongation (**Fig. 1.7b**). Films with 50% citric acid gave the best outcome in terms of the highest tensile strength and elongation (**Fig 1.7a and b**). This is probably due to the multiple hydroxyl and COOH groups of citric acid providing many inter/intramolecular interactions between starch, PVA and additives.[14]

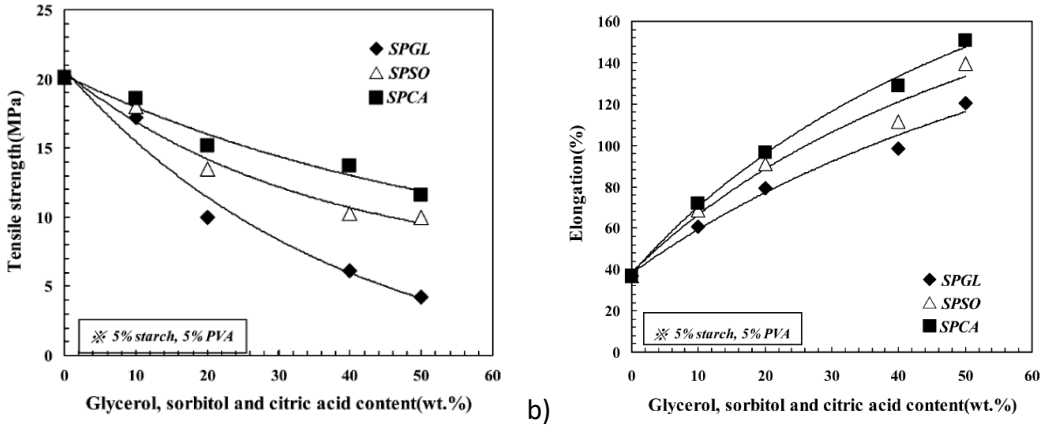

a) b)

Figure 1.7. a) The tensile strength of starch/PVA films prepared with glycerol (SPGL), sorbitol (SPSO) or citric acid (SPCA). b) The elongation of starch/PVA films prepared with glycerol (SPGL), sorbitol (SPSO) or citric acid (SPCA). [14]

1.9 Starch-based Wound Dressing

In the biomedical field starch has been utilized for a variety of tasks such as scaffolding for tissue engineering, and as a component in drug delivery systems and bone replacement implants. Starch, as one of the alternatives for biological wound dressing, suffers from high hydrophilic character and relatively poor mechanical properties. These weaknesses limit their applications for TRWDs. Starch-based films, however, can be further improved by cross-linking. Crosslinking can help to reduce the interaction between water and starch and improve its structural integrity. Common crosslinking agents are epichlorohydrin, glutaraldehyde and phosphoryl chloride. [15]

Cadexomer iodine (CI) is formed by crosslinking dextrin (low-molecular-weight carbohydrates produced by the hydrolysis of starch or glycogen) with epichlorohydrin in the presence of iodine (Scheme 1.4). The iodine is physically immobilized in the matrix without any chemical bonding. CI has high absorptive capacity: 1g of CI is able to absorb up to 7g of fluid. It is used as a wound dressing and is commercially available as an ointment or medicated sheet. When CI is applied to a wound, it absorbs fluids (such as exudate and pus) and swells. As it swells, it releases iodine slowly which results in a sustainable level of iodine in the wound bed to kill bacteria.[16] Unfortunately, it does have some side effects such as skin irritation, stains and allergic reaction. Also, it is not suitable for pregnant or lactating women because CI may pass to the baby through milk. [15]

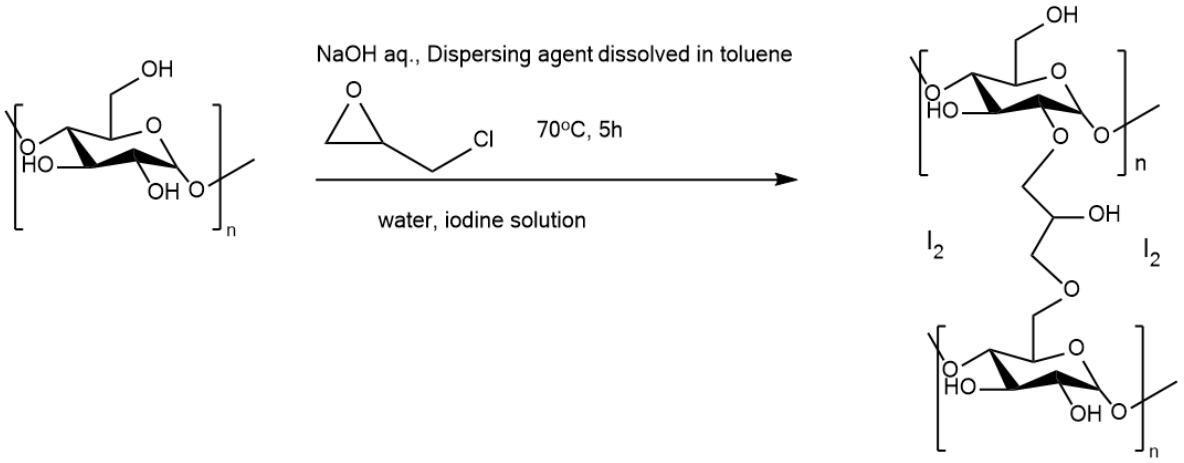

Scheme 1.4. Reaction Scheme of Cadexomer Iodine[17]

Sakchai et al introduced a chitosan-dextrin film by crosslinking chitosan and dextrin with glutaraldehyde. It showed improved mechanical properties and maintained water uptake level compared with chitosan alone. The films displayed good cell adhesion to pig intestine. Also, the addition of propylene glycol as plasticizer helped enhance its swelling ability and mechanical

properties.[18] However, it should be noted that glutaraldehyde is potentially harmful to the human body.

Maleic acid cross-linked starch-PVA hydrogel films (SMPs) have been reported by Pang et al (**Scheme 1.5**).[19] Maleic acid has been widely used as a food additive as it is non-toxic and biodegradable. It was found that the swelling capacity of the SMPs could be affected by precursor composition, purification methods, pH and temperature. More PVA leads to lower swelling ability due to higher crystallinity. Different morphologies were observed via different purification methods by TEM analysis. The direct precipitation of the SMP hydrogels generated a smooth surface morphology while the freeze-dried films showed a porous network structure, resulting in higher swelling ability. Also, optimum swelling ability can be achieved at 37 ^{o}C with pH 7. As the swelling ability can be manipulated by varying the amount of starch, maleic acid and PVA, these films could be used in wound dressing applications.[19]

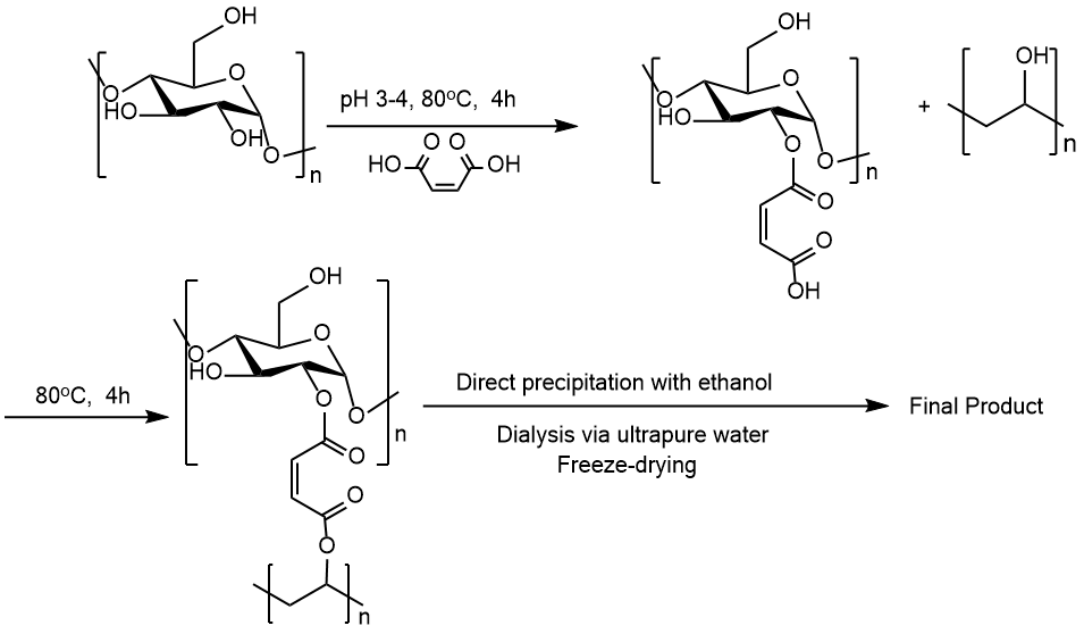

Scheme 1.5. Reaction Scheme of SMPs[19]

1.10 Thermoresponsive Starch

Unmodified starch is not TR. Recently, Ju et al have reported that TR starch can be obtained by reacting cooked starch with butyl glycidyl ether to obtain 2-hydroxy-3-butoxypropyl cooked starch (HBPS) (**Scheme 1.6**).[20]

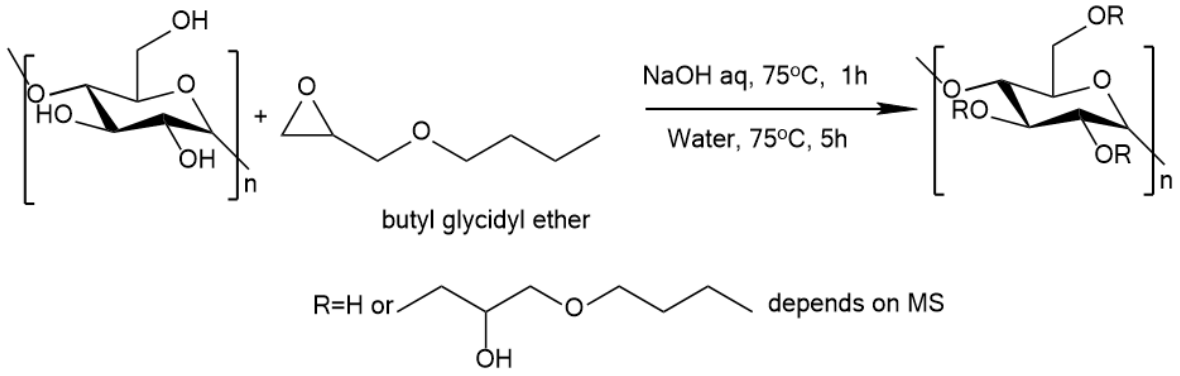

Scheme 1.6. Synthesis of HBPS[20]

The LCSTs of the HBPSs was determined by measuring the degree of light transmittance through an aqueous solution of the HBPSs at different temperatures (**Fig 1.8**). The HBPSs with molar substitutions (MSs) ranging from 0.32 to 0.63 displayed LCSTs ranging from 32.5 to 4.5 °C based on turbidity measurements. The LCST decreased as the molar substitution (MS) increased. Using pyrene as a probe, they were able to demonstrate that the HBPS forms micelles below the LCST and deformation of the micelles occurs above the LCST.

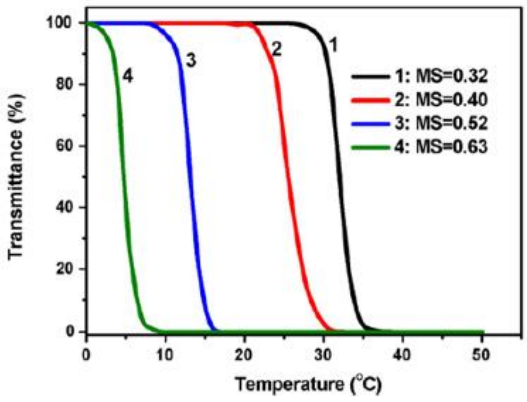

Figure 1.8. Light transmittance measurements of HBPS with MSs ranging from 0.32 to 0.63.[20]

In 2013, Ju et al. prepared TR 2-hydroxy3-isopropoxypropyl starches (HIPS), using Hylon V starch and isopropyl glycidyl ether (**Scheme 1.7**). They demonstrated that the T_c of the HIPS can be adjusted from 69 °C to 28 °C by varying the molar substitution. They also demonstrated that the T_c can be altered by addition of salts or alcohols.[21]

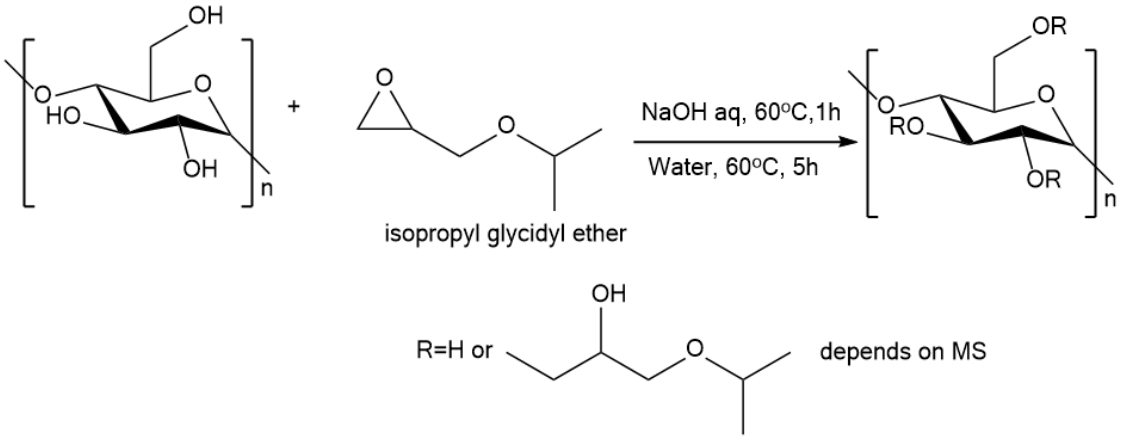

Scheme 1.7. Synthesis pathway of the thermoresponsive HIPS by Ju et al.[21]

Shortly thereafter, TR 3-[2-butoxy(ethoxy)$_m$]-2-hydroxypropyl starch ethers (BE$_m$S) (m = 0, 1, or 2) were developed by reacting degraded waxy maize starch with glycidyl ethers bearing oligo(ethylene glycol) spacers of various lengths (Scheme 1.8). It was found that the LCSTs of the BE$_m$Ss increased as the length of the oligo(ethylene glycol) spacer increased as a result of the

enhanced interaction between water molecules and the starch derivatives with longer pendants. However, the effects of salts and the concentration of BE_mS decreased when longer side chains were present.[22]

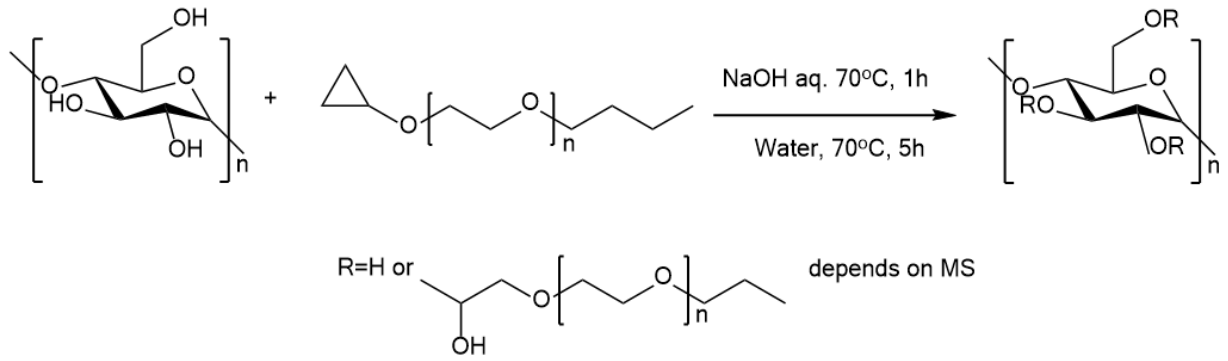

Scheme 1.8. Synthesis pathway of the thermoresponsive BEmS by Ju et al.[22]

Recently, a dual pH and TR tertiary amine starch ether (TAS) was synthesized by grafting dibutyl epoxy propylamine onto hydroxyethyl starch. The LCST could be tuned by varying the alkyl chain length, the average molar substitution (MS), and pH.[23]

1.11 Starch Nanoparticles

Nanoparticles are defined as particles being 10-1000 nanometers in size. For nanomaterials, size dependent properties are often observed in contrast with bulky materials. Starch nanoparticles (SNPs) can be prepared via three methods: hydrolysis, precipitation and mechanical treatment.[12] For the purposes of this research proposal, we are specifically focusing upon experimental grade SNPs prepared by Ecosynthetix Inc., a company in Burlington, Ontario, Canada.

1.12 TR Starch Nanoparticles

Magda Karski, a graduate student in the Taylor group at the University of Waterloo, has prepared TR SNPs. Experimental grade SNPs were used in this project. Karski reacted these SNPs with 1,2-butene oxide under basic conditions to give hydroxybutylated SNPs (abbreviated HBSNPs, **Scheme 1.9**).[24]

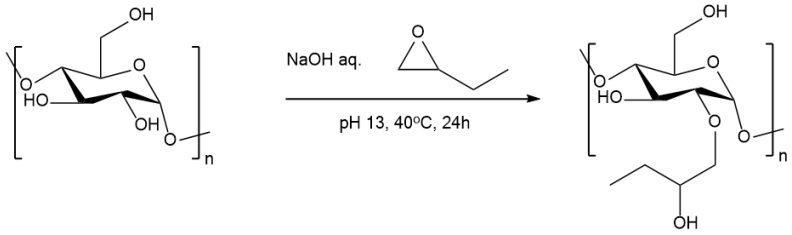

Scheme 1.9. Synthesis of TR HBSNPs[24]

It was found that the HBSNPs were TR if the molar substitution was greater than one as determined by measuring the degree of light transmittance through an aqueous solution of the HBSNPs at different temperatures (**Fig. 1.9**). The T_c decreased as the MS increases, which was consistent with the results of other TR starch materials mentioned above in **Section 1.10** (**Fig. 1.8**). The T_c can also be tuned by the addition of salts.[25]

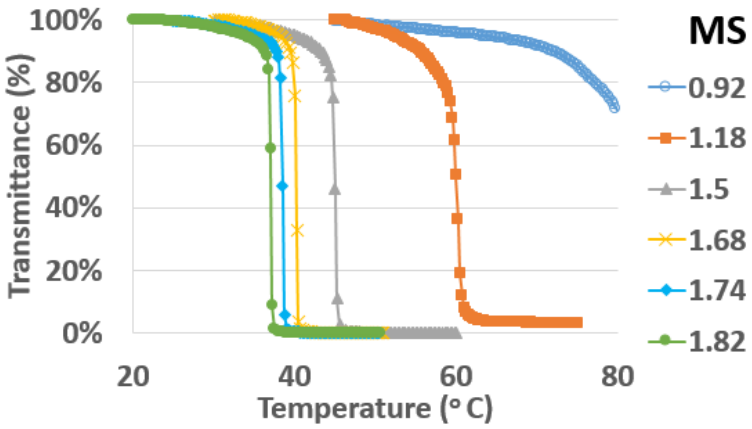

Figure 1.9. Light transmittance measurements of TR HBSNPs with MSs ranging from 0.92 to 1.82 (Zheng unpublished results).[25]

1.13 Research Objective

The objective of this thesis is to develop thermoresponsive starch or SNP films. The long term goal of this research is to develop thermoresponsive wound dressings based on starch or SNPs.

Chapter 2

2.1 HBSNP Films

We began our studies by attempting to make TR films from HBSNPs that were prepared from experimental SNPs from Ecosynthetix. All of the films prepared in this thesis were made by solution casting. HBSNP dispersions were prepared first. Subsequently, a certain amount of plasticizer, such as GY, was added and the dispersions were stirred overnight then cast on a silicone substrate and allowed to air dry. The resulting films were stored in a humidity controlled environmental chamber.

Films were initially made out of HBSNPs, with MSs ranging from 0.9 to 2.18, in the presence of 10 wt. % GY. It was observed that HBSNPs with higher MSs generated a more flexible film. However, if these films were left on the benchtop, they readily cracked due to loss of water or turned soft as they absorbed moisture depending upon the relative humidity (RH). Consequently, they had to be stored in an environmental chamber containing a saturated salt solution to create an environment with constant RH (60%RH) (**Fig. 2.1**). However, even when they were stored under these conditions, the HBSNP films eventually became brittle and cracked.

a)  b) 

Figure 2.1.a) An HBSNP (MS = 0.9) film made with 10 wt. % GY. b) An HBSNP (MS = 2.18) made with 10 wt. % GY.

Starch films made using a combination of 50 wt% of sorbitol and 50 wt% of GY have been shown to be quite stable (do not readily crack), transparent and flexible, even after 9 months storage at 25 ºC at 60% RH and 40 ºC at 75% RH.[26] Therefore, we attempted to prepare films from HBSNPs in the presence of varying amounts of sorbitol and GY. Unfortunately, this produced films that readily cracked (for an example see **Fig. 2.2b**). Using only sorbitol gave opaque films that also readily cracked (for an example see **Fig. 2.2a**).

a)  b) 

Figure 2.2. a) An HBSNP film prepared using 20 wt. % sorbitol. b) An HBSNP film prepared using 20 wt. % GY and 20 wt. % sorbitol.

2.2 HBSNP/PVA Blended Films

Although we were able to cast HBSNPs films using GY as plasticizer, they readily lost moisture and were relatively easy to break. One way to enhance the mechanical properties of starch films is to blend the starch with other polymers.[27] Polyvinyl alcohol (PVA) has good film-forming properties and ahesive properties. It has broad applications in paper coating, water soluble films and paper adhersive.[27] Park et al cast starch/PVA films using different additives such as GY, citric acid and sorbitol. The resulting films were less rigid resulting in lower tensile strength and higher elongation.[14]

The PVA selected for these studies was 87%-89% hydrolysed with an Mn of 89,000 g mol^{-1}. HBSNPs were blended with different amounts of PVA and GY. A 5 wt. % aqueous dispersion of PVA and a 5 wt. % aqueous dispersion of HBSNPs were prepared, mixed together along with GY, and then cast on the silicone substrate. The amount of PVA and GY used to make the films and the state (flexible or cracked) of the obtained film is given in **Table 2.1**. All films were opaque and yellowish. Most of the films were brittle and cracked under 24% RH or 60% RH. The minimum amount of GY and PVA that was required to create flexible, noncracking films was 40 wt.% GY and 40 wt.% PVA (wt.% is defined here as the wt of GY or PVA divided by the wt of HBSNP × 100%, also known as parts per hundred (pph)). Starch is normally blended into PVA films as a minor component to create more biodegradable materials.[28] In our case, due to the high content of HBSNPs with respect to PVA, the two polymers were not highly miscible resulting in opaque and cracked films.

Table 2.1. State of the HBSNP films prepared with various amount of GY and PVA

Entry	PVA (wt%)	GY (wt%)	State of the films	Entry	PVA (wt%)	GY (wt%)	State of the films
1	10	10	N[a]	9	30	10	N[a]
2	10	20	N[a]	10	30	20	N[a]
3	10	30	N[a]	11	30	30	N[a]
4	10	40	N[a]	12	30	40	N[a]
5	20	10	N[a]	13	40	10	N[a]
6	20	20	N[a]	14	40	20	N[a]
7	20	30	N[a]	15	40	30	N[a]
8	20	40	N[a]	16	40	40	P[b]

[a]N: Negative-films cracked.; [b]P: Positive-films were relatively flexible and did not readily crack.

a)  b) 

Figure 2.3. a) An HBSNP film prepared using with 40wt.% GY and 40wt.% PVA and stored under 60% RH; b) An HBSNP film prepared using with 10wt.% GY and 10wt.% PVA and stored under 60% RH.

2.2.1 Mechanical Properties of the HBSNP/PVA Films

To obtain films of even thickness, some of the cast HBSNP/PVA/GY films (**Table 2.2**) were compressed at 65 ^{o}C for 5 mins with a hot press. The mechanical properties of these films were examined by dynamic mechanical thermal analysis (DMTA) via tensile testing at ambient temperature.

Table 2.2. The relative amounts of HBSNP, PVA, and GY that were used to prepare HBSNP/PVA/GY films for tensile testing.

Entry	HBSNP:PVA:GY[a]	HBSNP fraction(wt%)[b]	PVA fraction (wt%)[b]	GY fraction (wt%)[b]
1	10:4:4	56	22	22
2	10:5:5	50	25	25
3	10:6:6	45	27.5	27.5

[a] HBSNP:PVA:GY:the ratios were defined by weight. The amount of PVA and GY were represented as parts per hundred (pph).
[b] HBSNP fraction(wt%),PVA fraction(wt%), GYfraction(wt%): The fractions were defined as the weight precent over the total mass.

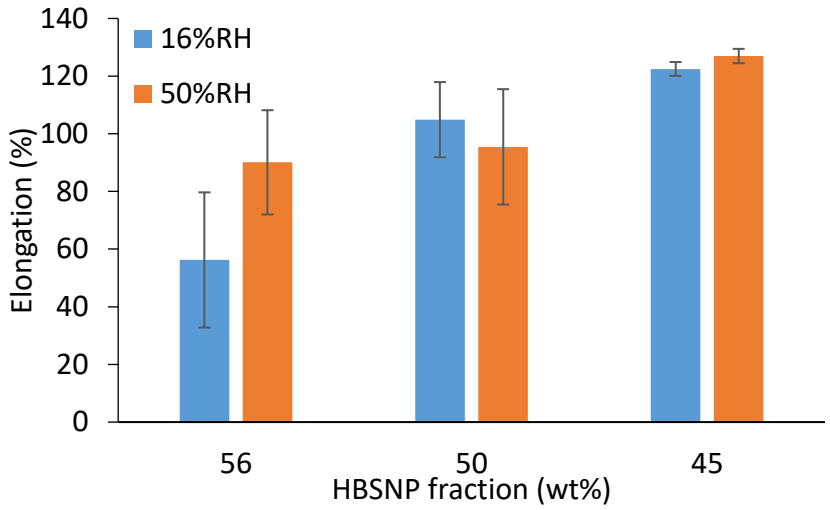

a)

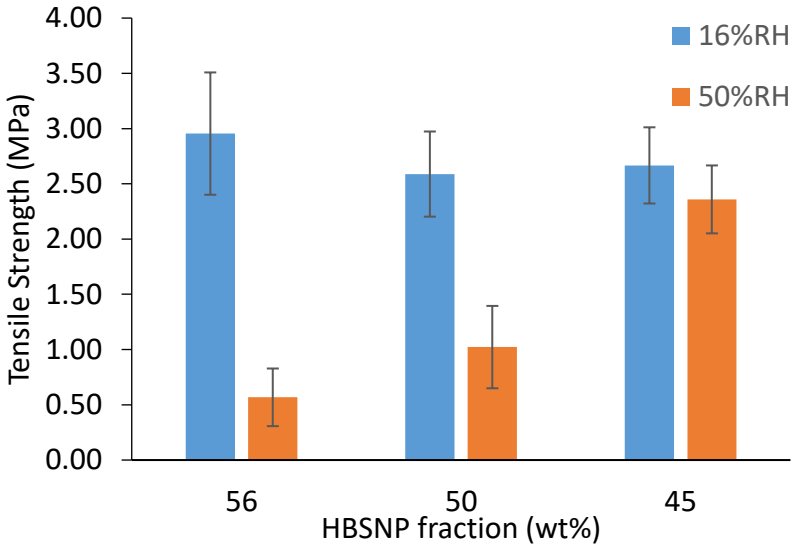

b)

Figure 2.4. a) The tensile strength of HBSNPs films cast with different amounts of PVA and GY (see **Table 2.2** for amounts). b) The elongation of HBSNPs films cast with different amounts of PVA and GY (see **Table 2.2** for amounts).

It was found that under 16% RH, the films showed no significant difference in tensile strength while under 50% RH, the tensile strength increased with PVA content (**Fig. 2.4a**). For elongation, films with higher PVA content can be extended longer (**Fig. 2.4b**). It appears that PVA helped to enhance the mechanical properties of the HBSNP films in terms of tensile strength and elongation. This was not unexpected as PVA films themselves are known to have a high tensile strength and good flexibility while neat starch films are brittle. Consequently, the addition of PVA

in the starch films yielded films with better mechanical properties.[29] There are three phases in blended polymers: dispersed phase, continuous phase and interface phase. The interface phase plays an important role in defining their mechanical properties. Interfacial interactions between HBSNPs and PVA most likely involves strong H-bonding. Such strong interfacial interactions can mimimize slip between the matrix and other components.[30]

Elastic modulus describes how easily a material can be stretched. With respect to elastic modulus, films stored under 50% RH were relatively ductile (lower elastic modulus) while HBSNPs films turned stiffer (higher elastic modulus) under 16% RH (**Fig. 2.5**). As water also acted as a plasticizer, films stored under 50% RH were expected to have a higher moisture content thus the mobility of the polymers were improved, resulting in a lower elastic modulus.[29]

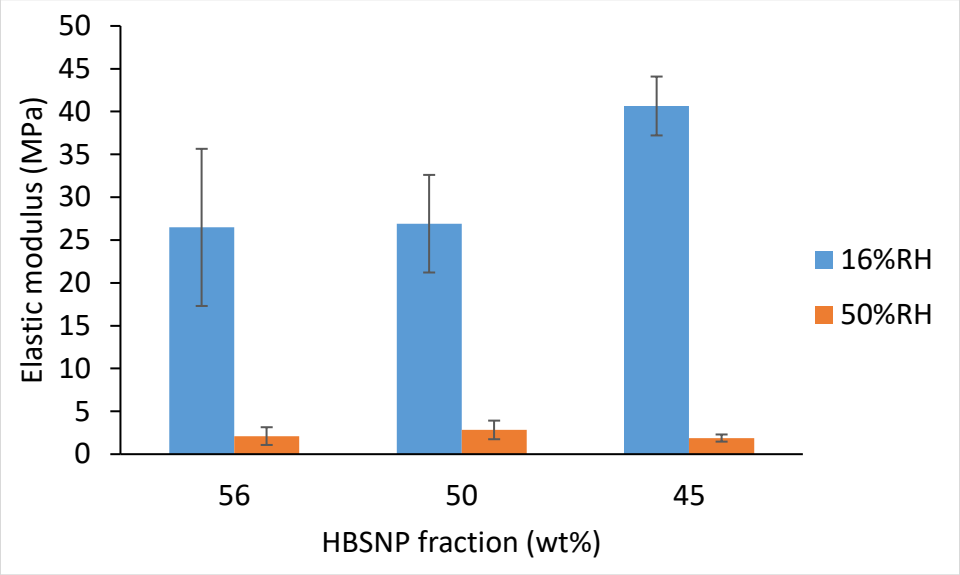

Figure 2.5. Elastic modulus versus HBSNP content in HBSNP/PVA/GY films.

The HBSNPs films turned stiffer (higher elastic modulus) with PVA applied under 16%RH, which was also reported by Tian et al,[29] while there is no significant difference between the films stored under 50%RH. This is probably due to the moisture content. Under 50% RH,

more water is retained in the films. The intefacial interactions (hydrogen bonding) between PVA and HBSNPs somehow became weaker even with more PVA content.

2.2.2 Thermoresponsivity Study

Thermoresponsivity of films can be evaluated using differential scanning calorimetry (DSC). As introduced in **Section 1.5**, the hydrated thermoresponsive films exhibit an endothermic peak in the thermogram during the heating process, indicating that they undergo a thermal transition.[2] Before examining films using DSC, HBSNP aqueous dispersions of various concentrations were evaluated first (**Fig. 2.6**). Compared with the thermogram of pNIPAAM aqueous dispersions (**Fig. 2.7**), the thermogram of the HBSNPs aqueous dispersions showed only a minimal amount of heat absorbed that is scarcely detected during the heating process.

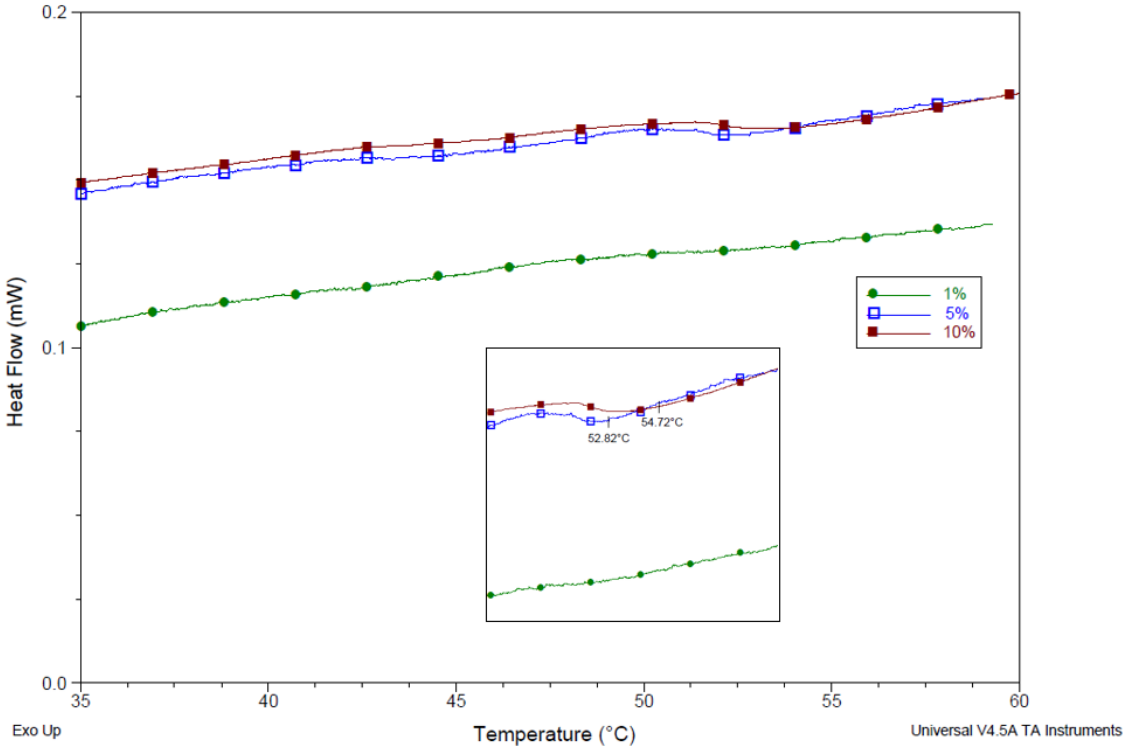

Figure 2.6. DSC thermogram of HBSNPs (MS = 1.3, LCST = 50 ºC by light transmittance) aqueous dispersions with concentrations varying from 1% to 10%.

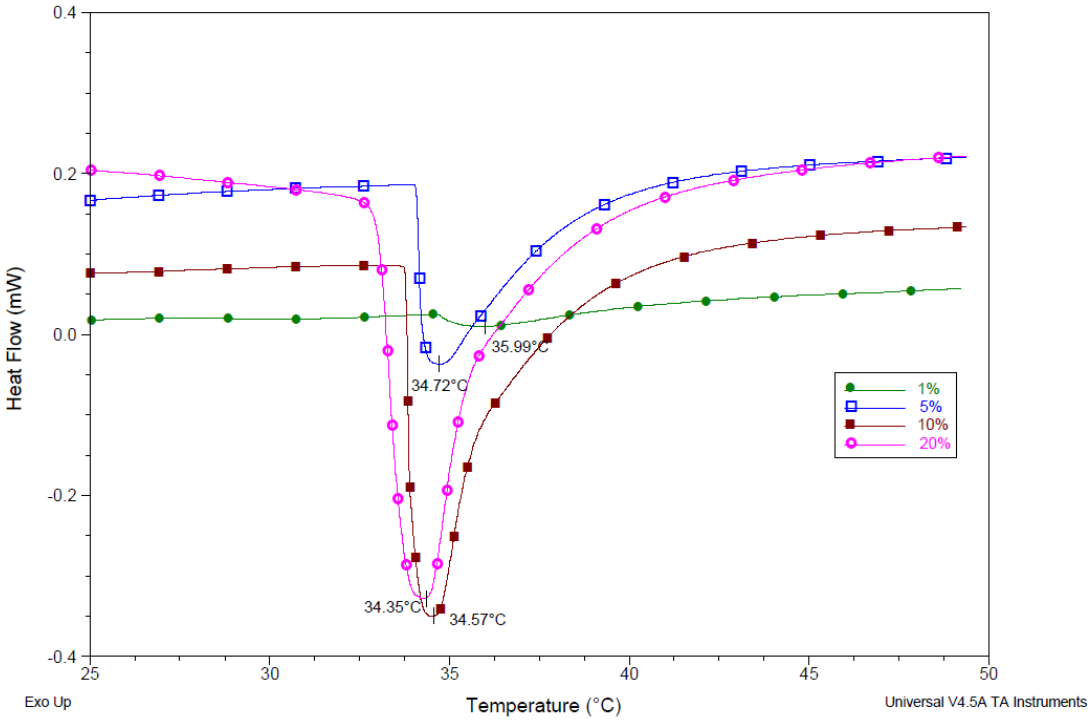

Figure 2.7. DSC thermogram of pNIPAAM aqueous dispersions with concentrations varying from 1% to 20%

The thermoresponsivity of the HBSNP/PVA/GY films was also studied. Concentrated aqueous mixtures of the films were stirred overnight which yielded gel-state dispersions. No thermal transition was observed (**Fig. 2.8**).

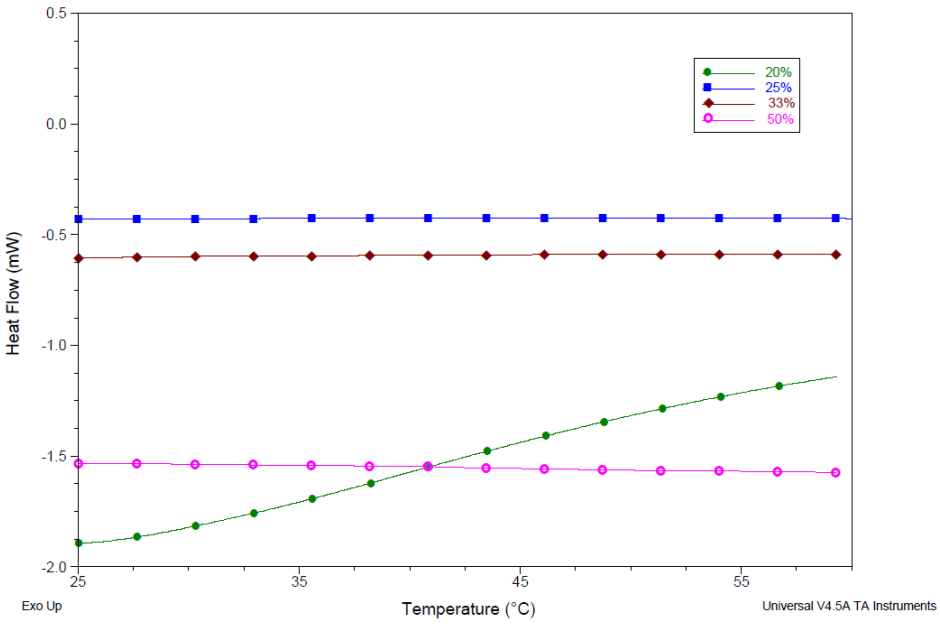

Figure 2.8. Thermogram of HBSNP/PVA/GY film which consists of 50wt%HBSNPs, 25wt%PVA and 25wt%GY. Aqueous dispersions of different concentrations were examined via DSC measurement.

Although HBSNP/PVA/GY blended films had some desirable mechanical properties, they were not thermoresponsive and not completely bio-based.

2.3 Poly(ethylene glycol) grafted HBSNPs

Cast starch films tend to crack when the water evaporates from the films. Although the films can be somewhat stabilized by using other plasticizers, such as GY, GY can migrate which can again result in brittle films even when stored under controlled humidity conditions. To decrease the sensitivity to any environmental humidity change, apart from using other plasticizers, poly(ethylene glycol) (PEG) grafted HBSNPs were prepared. Nasim and Peyman showed that by grafting methoxy PEG (mPEG) onto starch, the T_gs of the resulting material decreased as the mPEG chains got longer providing a more flexible polymer material. The grafted PEG increased the space between each adjacent polymer chains which allowed the polymer chains to slide easily under stretching, resulting in a lower T_g.[31]

2.3.1 Synthesis of Poly(ethylene glycol) grafted HBSNPs

We first attempted to attach PEG to HBSNPs by attaching mPEG (Mn 2000 g mol^{-1}) to the HBSNPs via a succinic acid linker according to the procedure of Wang et al, who attached mPEG to starch using maleic anhydride as a coupling agent. [32] Thus mPEG was reacted with succinic anhydride in toluene at 110 ^{o}C for 2 hours (**Scheme 2.1**). HBSNPs (MS = 1.26, LCST = 50 ^{o}C) were then added to the reaction mixture and the water produced was removed by azeotropic distillation over a period of 2h. The reaction mixture was biphasic. After cooling, the reaction mixture was filtered, dialyzed and freeze-dried. However, no peak for the methyl protons on mPEG appeared in the NMR spectrum. The reaction efficiency was probably very low as a result of the heterogenous reaction conditions.

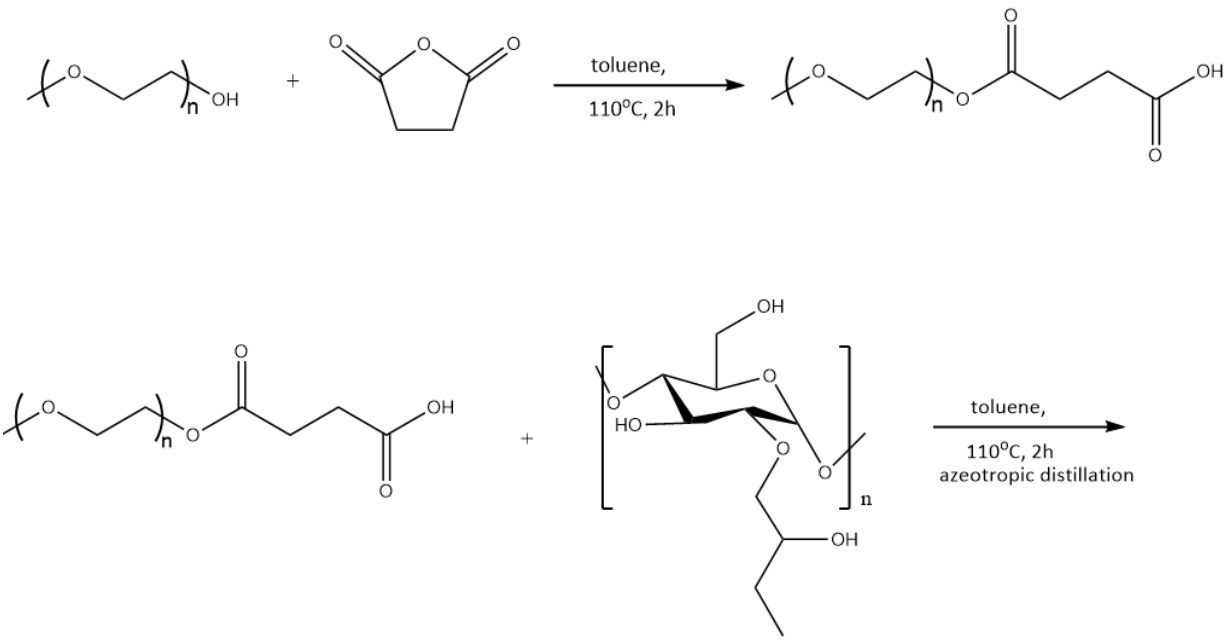

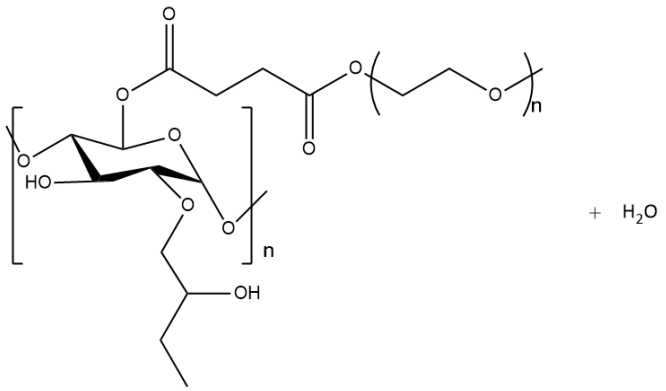

Scheme 2.1. The reaction scheme for the preparation of mPEG grafted HBSNPs using succinic anhydride as the linker.

We also attempted to prepare the succinic acid adduct of mPEG by reacting mPEG with succinic anhydride in the presence of 4-dimethylaminopyridine (DMAP) according to the procedure proposed by Yang et al. (**Scheme 2.2**).[33] The reaction mixture was precipitated in diethyl ether, dried and then examined by ^{1}H-NMR. However, only a 25% reaction efficiency was achieved as determined by ^{1}H-NMR spectroscopy. Here, the peak at 3.28 ppm is assigned to the methyl protons and the peak at 3.10 ppm corresponds to the methylene protons of the carboxylate. (**Fig 2.9**). Therefore, we decided to look at other approaches for attaching mPEG to the HBSNPs.

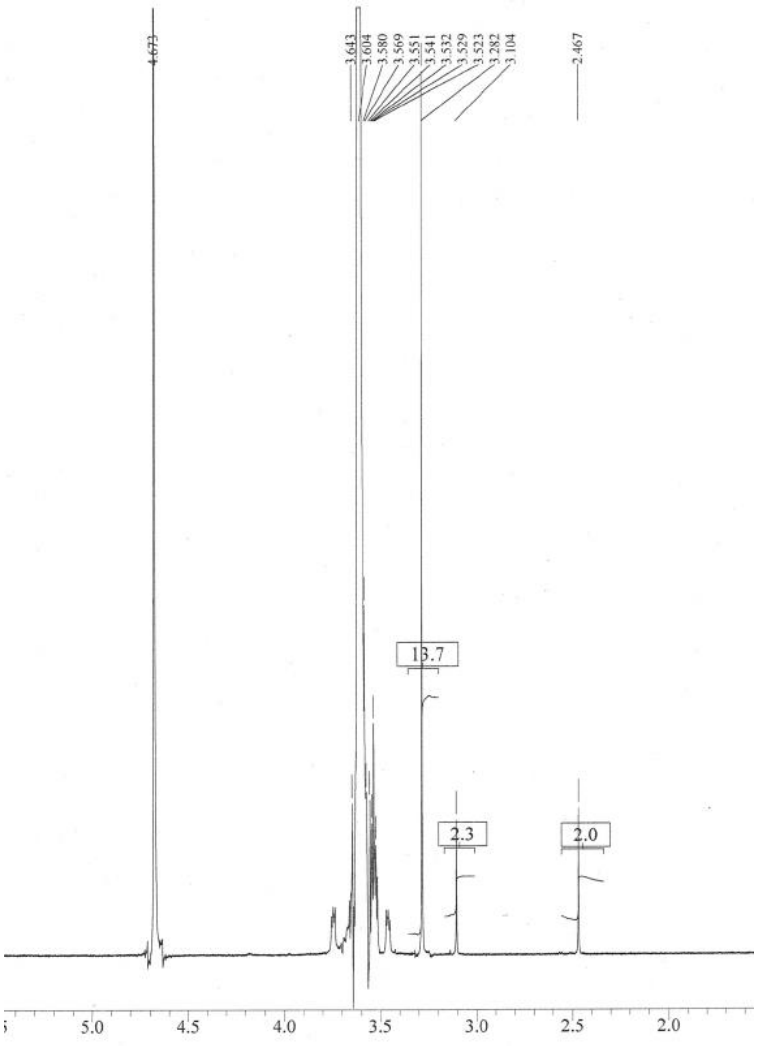

Figure 2.9. ^{1}H NMR spectrum of succinic acid adduct of mPEG in D_2O.

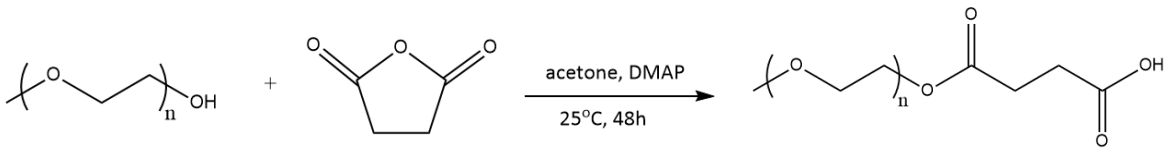

Scheme 2.2. Synthesis of mPEG carboxylate using DMAP.[33]

We prepared mPEG carboxylate (mPEG-COOH) by oxidizing the hydroxyl group of mPEG (Mn 2000) with chromium trioxide and sulfuric acid (Jones reagent) in DW (**Scheme 2.3**).[34] The crude product was extracted using methylene chloride and the mPEG-COOH was obtained by precipitation in ether.

The ^{1}H-NMR spectrum of the mPEG-COOH is shown in **Fig. 2.10**. The peak at 4 ppm was assigned to the methylene protons of the carboxylate and the peak at 3.2 ppm was assigned to the methyl protons. Theoretically, the ratio between these two peaks is 2:3 rather than 2.8:3. Meanwhile, the ratio between the hydroxy group (12.4 ppm-12.8 ppm) and the methyl group is 0.9:3, very close to 1:3. One possible reason is that the mPEG degraded to give PEG with two free hydroxy groups which were converted into carboxylates later.

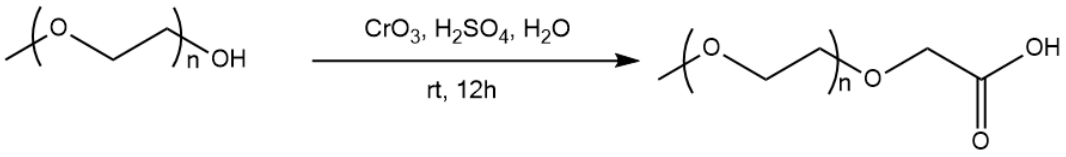

Scheme 2.3. Synthesis of mPEG-COOH by oxidation using chromium trioxide and sulfuric acid[34]

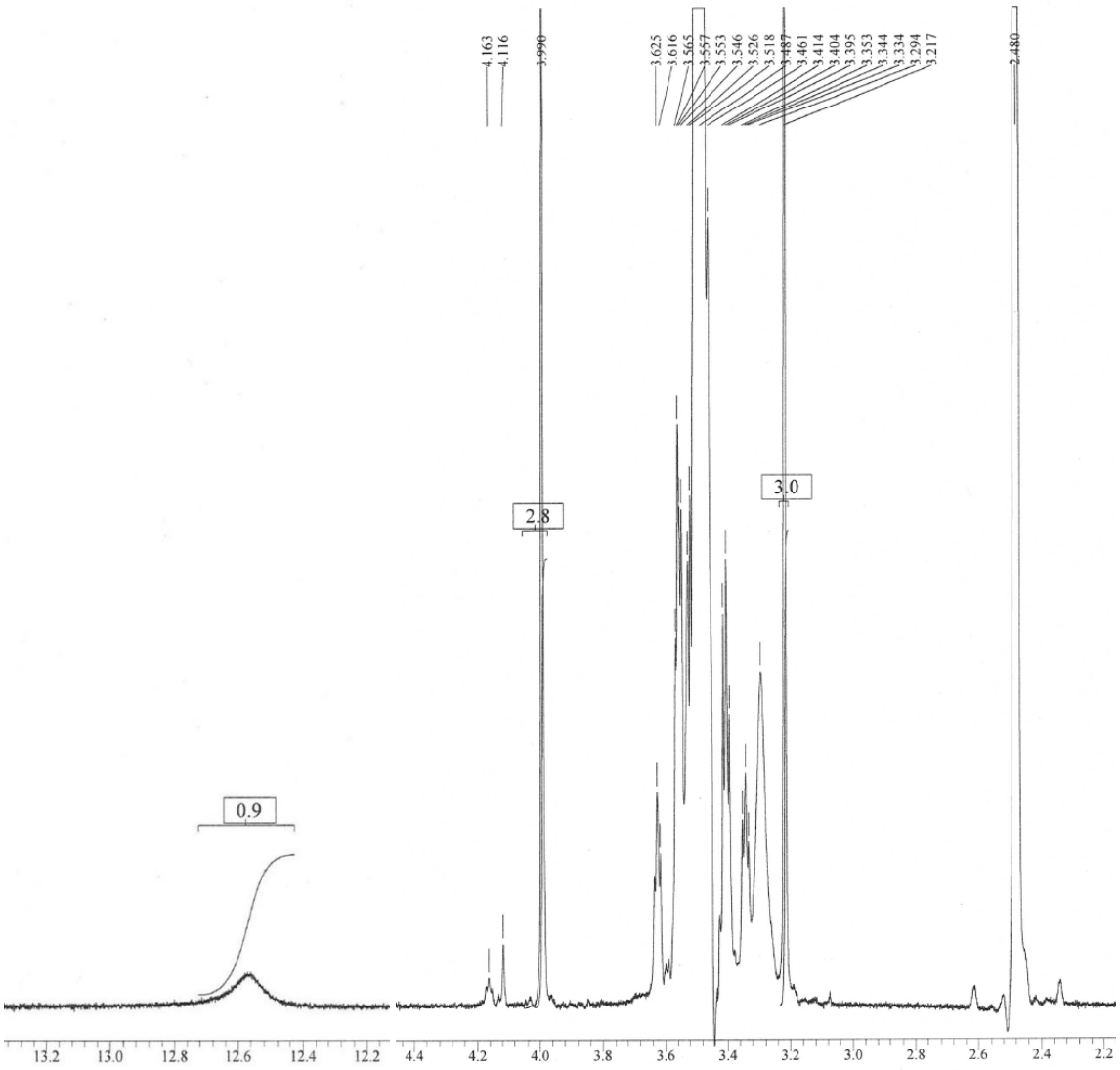

Figure 2.10. The ^{1}H-NMR spectrum of mPEG-COOH in deuterated DMSO.

The MALDI-TOF mass spectra of mPEG and the mPEG-COOH are shown in **Fig. 2.11.** Compared with mPEG, there are two main populations for mPEG-COOH, accounting for 92.1% of the total material. The smaller population is due to sodium adducts. It is possible that the mPEG underwent degradation as there are also small peaks appearing from 1200 to 1800 Da.

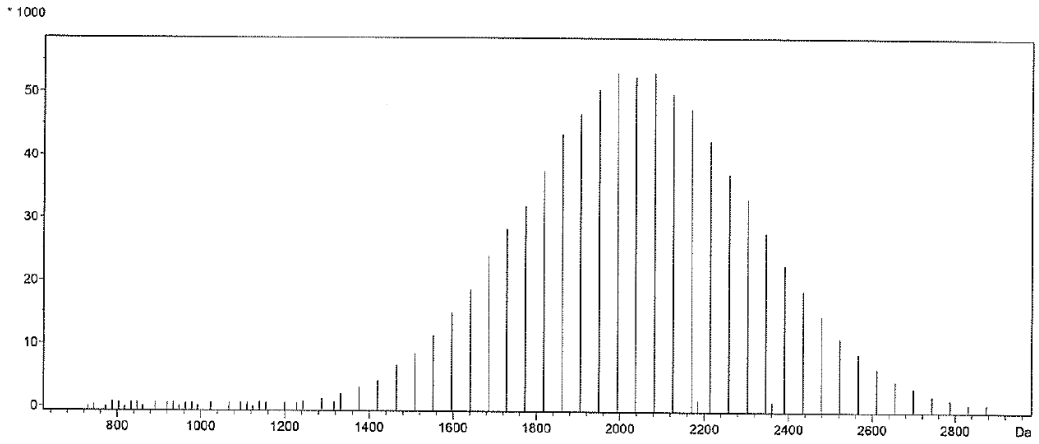

n	ser.	rep.unit	resid.	end1	end2	cation	Mn	Mw	pd	DP	% I.	cnt
1	1	PEG	-0.31104	OH	CH3	Na	2002.50	2047.61	1.02253	45.4570	97.6	48

a)

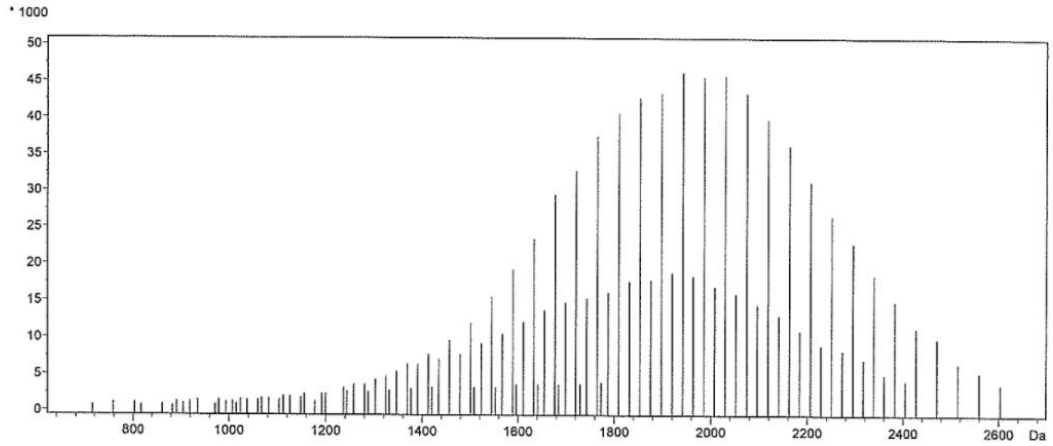

n	ser.	rep.unit	resid.	end1	end2	cation	Mn	Mw	pd	DP	% I.	cnt
1	1	PEG	-0.13208	75.0434	CH3	H	1935.37	1980.75	1.02345	43.9331	65.2	38
2	2	PEG	-0.13941	75.0434	CH3	Na	1835.10	1876.86	1.02275	41.6570	26.9	27

b)

Figure 2.11. MALDI-TOF mass spectra of a) mPEG and b) mPEG-COOH.

The mPEG-COOH was grafted onto the HBSNPs (MS = 1.26, LCST = 50 ^{o}C) using 1-ethyl-3-(3-dimethylaminopropyl) carbodiimide (EDC) and catalytic amount of DMAP at rt for 2 days in DMSO (**Scheme 2.4**).[35] The product was subjected to dialysis against DW using a dialysis bag with MW cut-off of 100 kD. After dialysis, the mixture was lyophilized to give a white-powder. The yield was 62%.

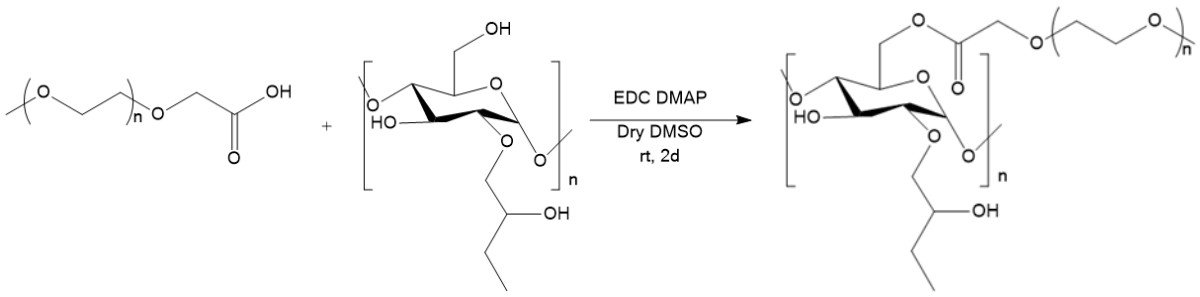

Scheme 2.4. Coupling of mPEG to HBSNPs (MS 1.26) using EDC and DMAP.[35]

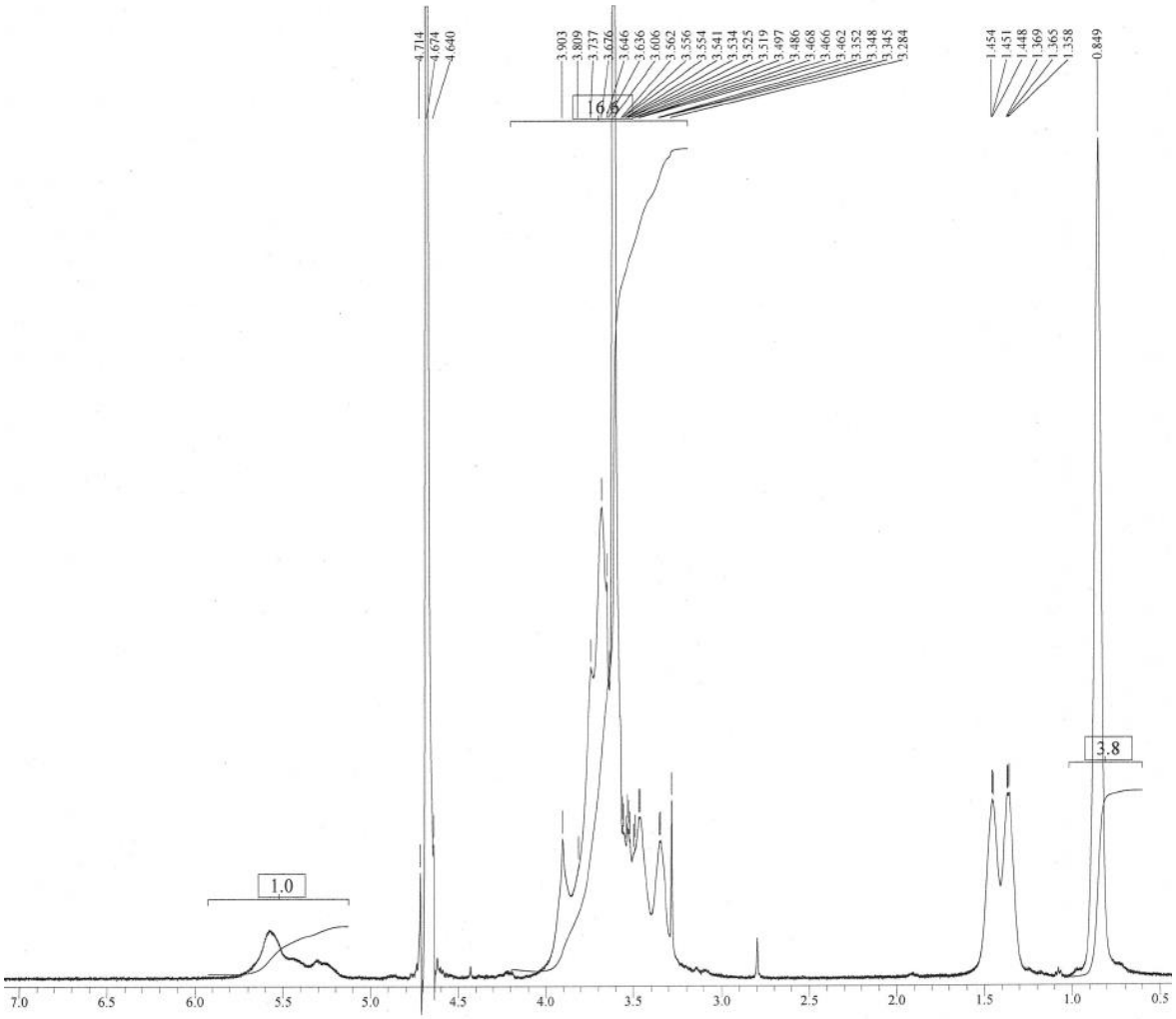

Figure 2.12. ^{1}H NMR spectrum of 0.05 eq. mPEG grafted HBSNPs in D_2O.

The ^{1}H-NMR spectrum of the product is shown in **Fig. 2.12**. The reaction efficiency was estimated as 78% for the reaction with 0.05 eq. of mPEG-COOH as determined by calculating the

integral of methylene protons of mPEG from the spectrum over the theoretical integral of methylene protons of added mPEG-COOH (See **Section 5.5**).

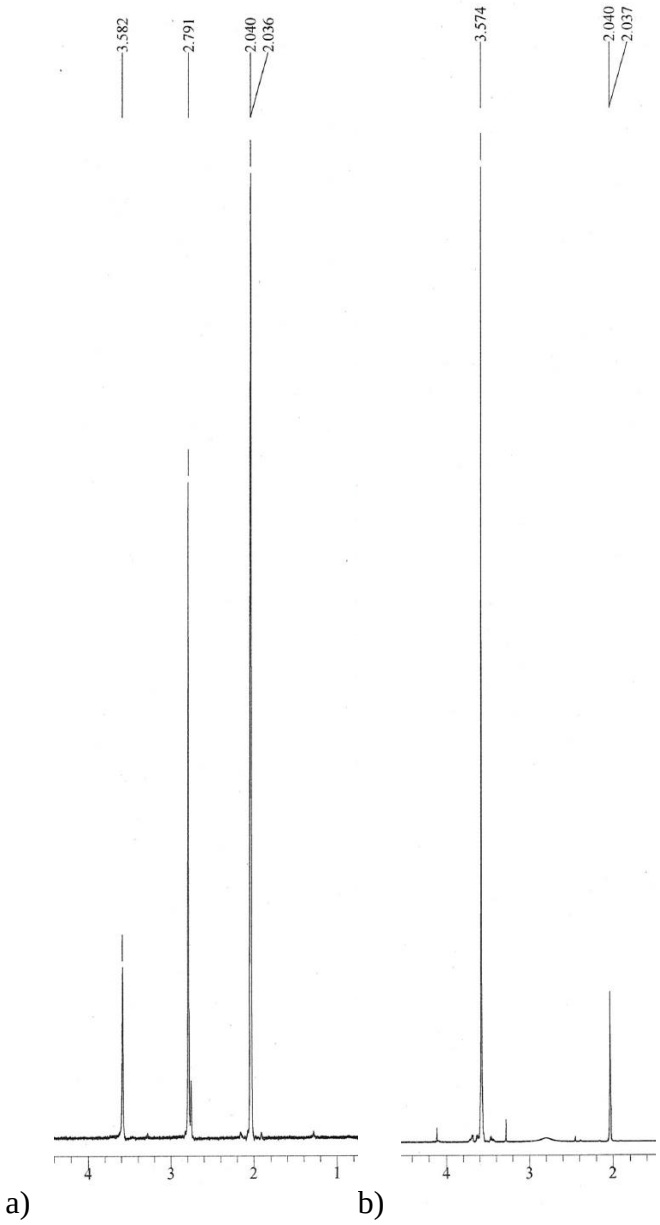

Figure 2.13. ^{1}H-NMR spectra of a) deuterated acetone washing of the mPEG-HBSNPs, and b) the same as (a) except spiked with mPEG-COOH.

Although the ^{1}H-NMR spectrum of the mPEG grafted HBSNPs suggested that the mPEG was indeed grafted onto the SNPs, it is possible that not all of it was grafted and that some of the

additional peaks in the NMR spectrum were due to unreacted mPEG-COOH. To determine if the unreacted mPEG-COOH was removed completely, the product was washed with deuterated acetone as any remaining unreacted mPEG-COOH would dissolve in deuterated acetone and a ^{1}H-NMR spectrum of the washings was obtained (**Fig 2.13 A**). The peak at 3.58 ppm was assigned as the methylene protons of mPEG. This was confirmed by spiking the sample with mPEG-COOH (**Fig 2.13 B**). The intensity of the peak at 3.57 ppm increased, indicating the presence of residual mPEG-COOH in the washings and that not all of the mPEG-COOH was removed by dialysis. We were unable to remove all of the unreacted mPEG-COOH by dialysis.

2.3.2 Thermoresponsive Behavior Studies of mPEG grafted HBSNPs

The thermoresponsive behavior of the mPEG-HBSNPs was determined. The dispersibility of the mPEG-HBSNPs decreased compared with HBSNPs (**Fig. 2.13**). Nevertheless, all of the mPEG-HBSNPs were thermoresponsive. As more mPEG was grafted onto the HBSNPs, the resulting polymer became more hydrophilic and the LCST increased. The transmittance, instead of going down sharply to 0 %, decreased slowly. For mPEG-HBSNPs made with 0.4 eq. of mPEG-COOH, the transmittance decreased very slowly between 25-65 ^{o}C and then more rapidly from 65-75 ^{o}C. At 75 ^{o}C they appeared to stabilize at 20% transmittance (**Fig 2.14**). Instead of precipitating out of the dispersion, the mPEG-HBSNPs formed probably a micellar structure, which was also reported by Zhang et al.[35]

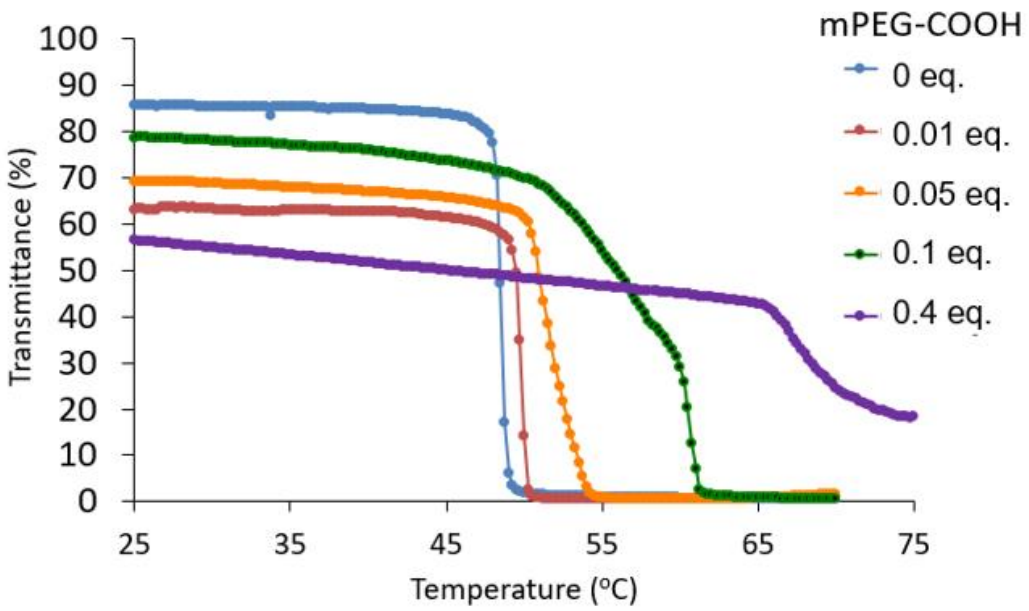

Figure 2.14. Light transmittance curves for aqueous dispersions (10g/L) of different eq. mPEG grafted HBSNPs (MS of the HB group = 1.26) using DW as reference.

We also noted that, upon cooling, the transmittance of the mPEG-HBSNPs increased and their LCSTs increased, as shown for the mPEG (0.05 eq.)-HBSNP in **Fig 2.15**. This indicates that the mPEG-HBSNPs required heating to be more dispersible.

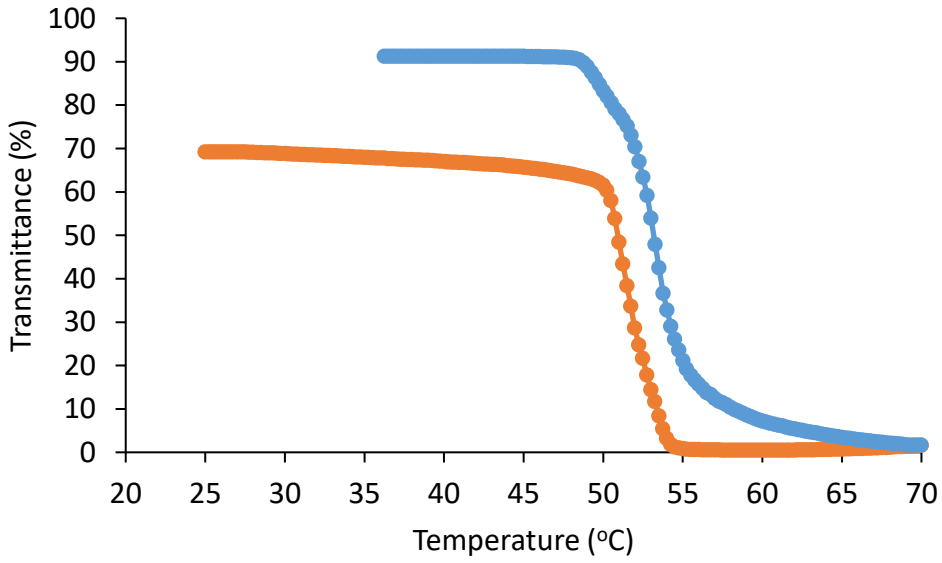

Figure 2.15. Light transmittance curves of HBSNPs grafted with 0.05 eq mPEG-COOH during the heating (red curve) and cooling (blue curve) process.

As there was a possibility that there was ungrafted mPEG-COOH present in the mPEG-HBSNPs, we examined the effect of free mPEG-COOH on the LCST of an HBSNP (MS = 1.26, LCST = 50 ºC). As is shown in **Fig2.16**, the addition of mPEG-COOH did not affect the LCST of the HBSNP.

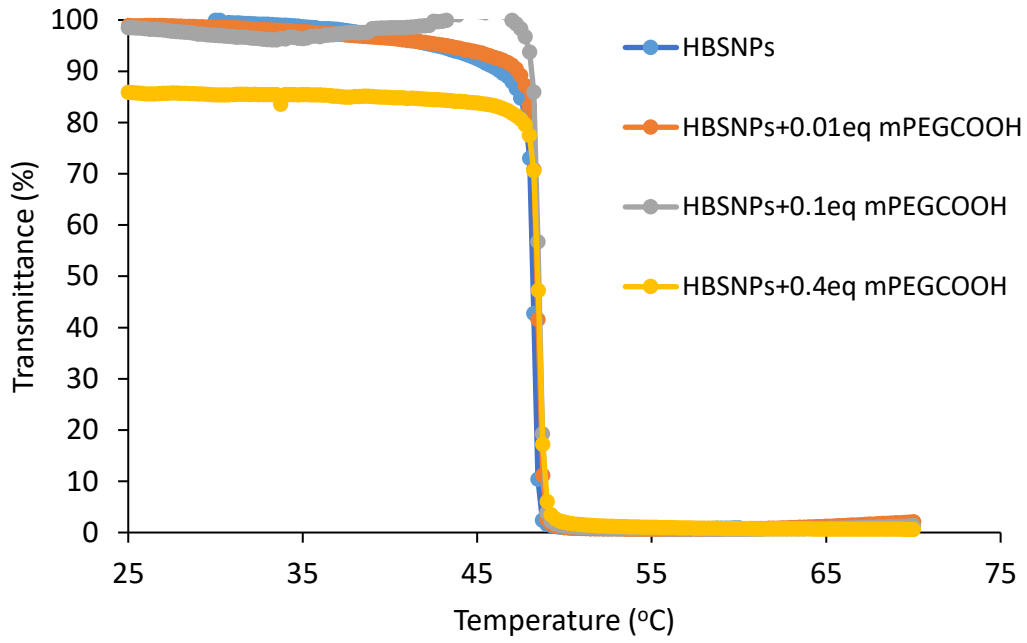

Figure 2.16. Light transmittance of HBSNPs dispersions (MS = 1.26) in the presence of various amounts of free mPEG-COOH.

The PEG-grafted HBSNPs were not pursued further due to purification issues (unreacted mPEG-COOH could not be removed completely) and the high cost for large scale production as EDC and mPEG are relatively pricy.

2.4 Hydroxybutylated Corn Starch based Nanocomposites

Nanofillers gather much attention for their ability to reinforce films .[8] For example, Ma et al prepared pea starch films reinforced with citric acid crosslinked SNPs. The introduction of the SNPs greatly improved the tensile strength and elastic modulus of the films.[36] This led us to

determine if incorporating SNPs in hydroxybutylated corn starch (HBCS) films would affect the physical properties of the films. Before preparing the nanocomposites, we compared the HBCS films and HBSNP films specifically in terms of tensile strength and elongation.

We began these studies by preparing films using hydroxybutylated corn starch (HBCS, MS = 1.89, LCST = 31 ^{o}C) and 10 wt. % GY and compared their mechanical properties to those of films prepared using the HBSNPs (MS = 1.82, LCST =33.5 ^{o}C) and 10 wt. % GY. The HBSNPs used in this study were derived from experimental SNPs. The HBCS films were relatively tougher in terms of higher tensile strength compared with HBSNP films while not showing much difference in elongation (**Fig. 2.5**). The HBCS is expected to have a higher molecular weight (MW) compared with HBSNP and MW is one of the factors greatly influencing the mechanical properties of polymers. Polymers with higher MW usually exhibit higher tensile strength and elongation.[37]

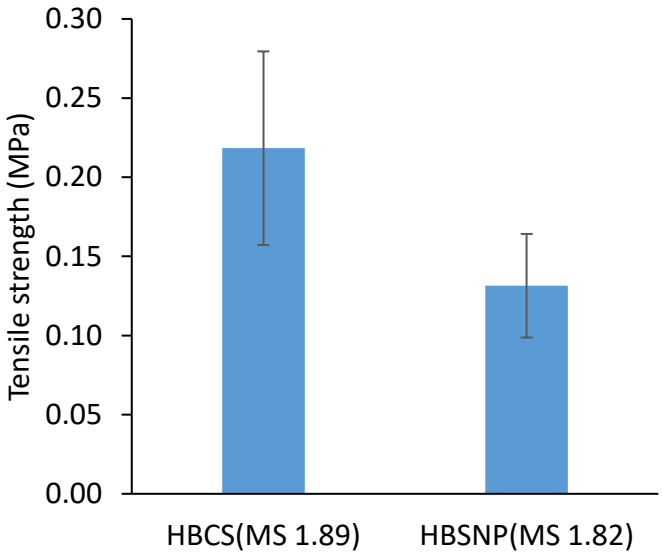

a)

b)

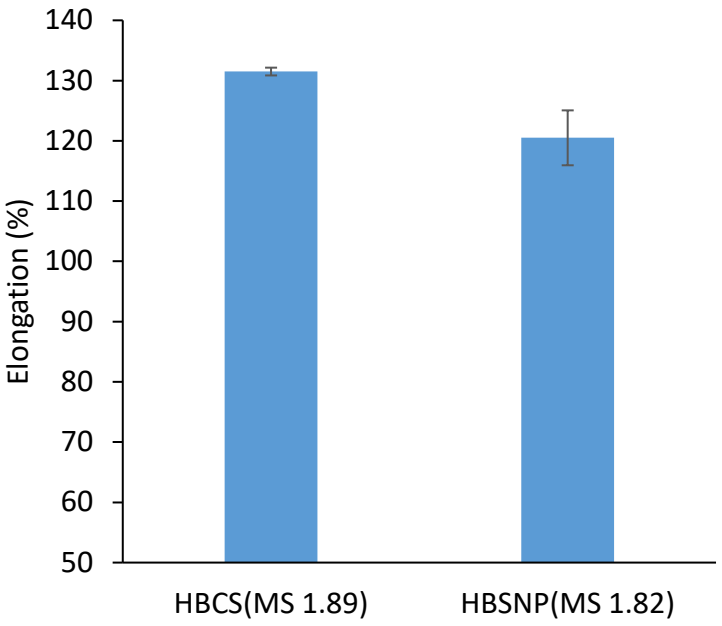

Figure 2.17. Tensile strength (a) and elongation (b) of an HBCS film and an HBSNP film prepared using 10 wt. % GY as plasticizer.

Based on the fact that HBCS films behave better than HBSNPs films, we examined SNPs as a filler for HBCS films. Various amounts of the SNPs (0 to 20 wt. %) and 10 wt.% GY was added to a 5 wt. % HBCS dispersion and stirred overnight. The mixtures were cast and allowed to air dry. The resulting films are henceforth referred to as SNP/HBCS films.

2.4.1 Mechanical Properties of HBCS-based Nanocomposites

All the samples were conditioned in a humidity chamber (50% RH) for at least two days before mechanical testing. The SNP/HBCS films showed a significant improvement in tensile strength from 0.23 MPa to 2.03 MPa (**Fig 2.18 a**). As nanocomposites are usually the stronger component to reinforce the matrix, SNPs are probably stiffer than HBCS in terms of higher crystallinity as the HBCS was prepared under base treatment at 40 ^{o}C for 24 h.[8] The elongation decreased significantly with addition of the SNPs from 130% to 59% (**Fig 2.18 b**). With more

SNPs incorporated, the films became much stiffer as the elastic modulus increased from 0.5 to 24.8MPa (**Fig 2.18 c**).

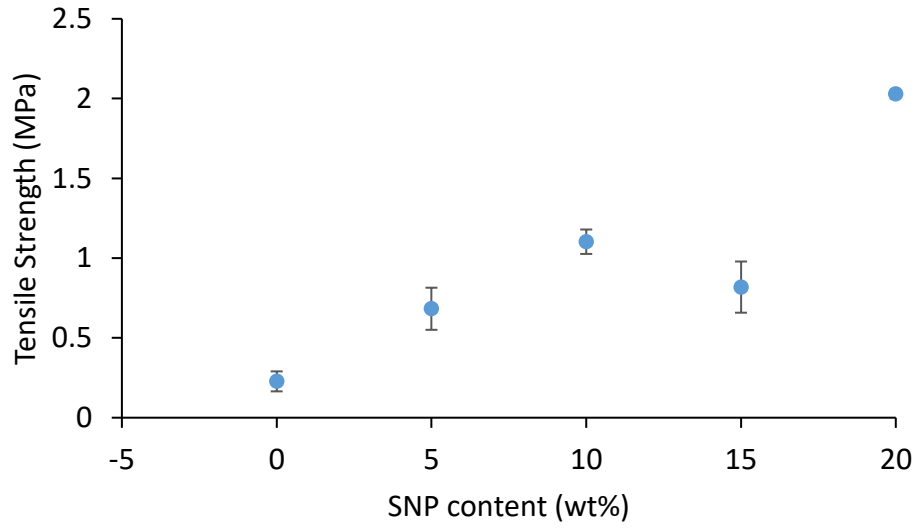

a)

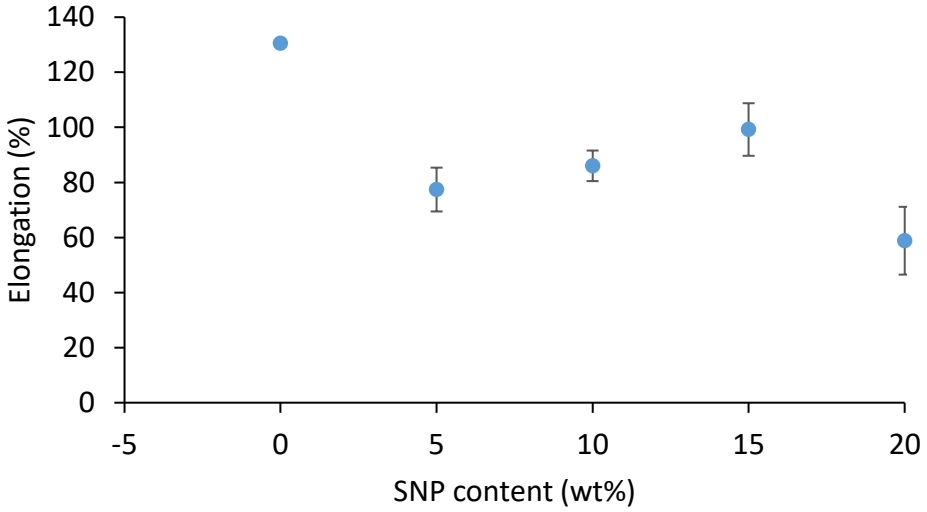

b)

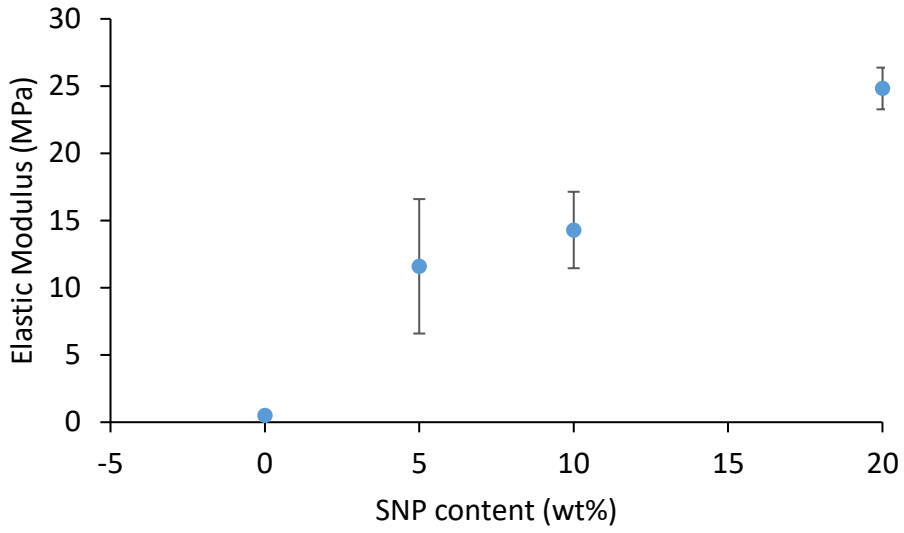

c)

Figure 2.18. The a) tensile strength, b) elongation and, c) elastic modulus of HBCS films reinforced with different amounts of SNPs.

SNPs incorporated into CS films (no HB group) were also prepared to determine how much the HB group affected the mechanical properties of the SNP/HBCS films. After gelatinizing corn starch (5 wt. % in DW) at 90 ^{o}C for 30 mins and cooling to rt, SNPs (0 - 20 wt. %) and GY (10 wt. %) were added. After stirring overnight, they were poured onto a silicone substrate and air dried. For these SNP/CS films, incorporating less than 10 wt. % SNPs helped to enhance their mechanical properties in terms of greater tensile strength, slightly increased elongation and greater elastic modulus (**Fig 2.19 a-c**). The reinforcement effect was attributed to the good interfacial interactions between the SNPs and the starch matrix.[36] Adding more than 10 wt. % of the SNPs had the opposite effect on the films. Compared with SNPs/HBCS films, the SNPs were probably not as stiff as the major component (cooked corn starch) in SNP/CS films to improve the mechanical properties of CS films.

Comparing the SNP/HBCS films to the SNP/CS films, the SNPs were more effective in improving the physical properties of HBCS films. In terms of wound dressing applications, only a low mount of SNPs is required to generate the necessary extension.

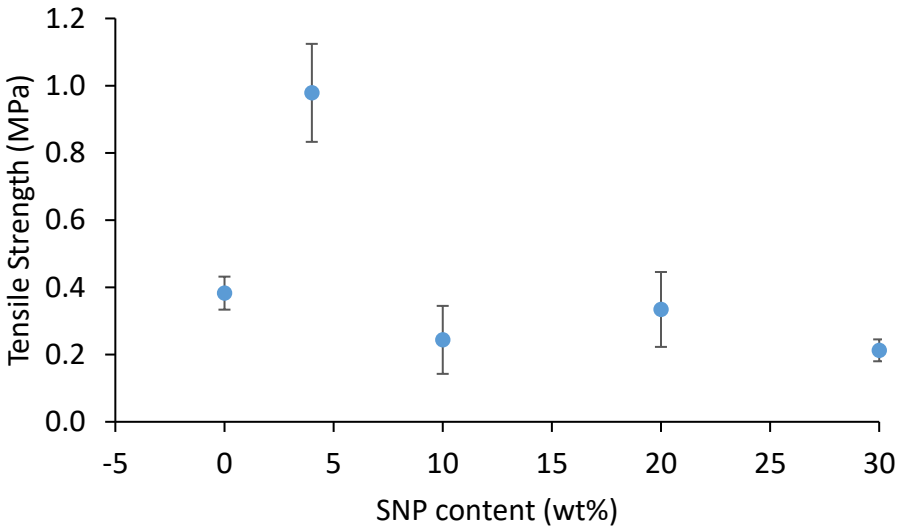

a)

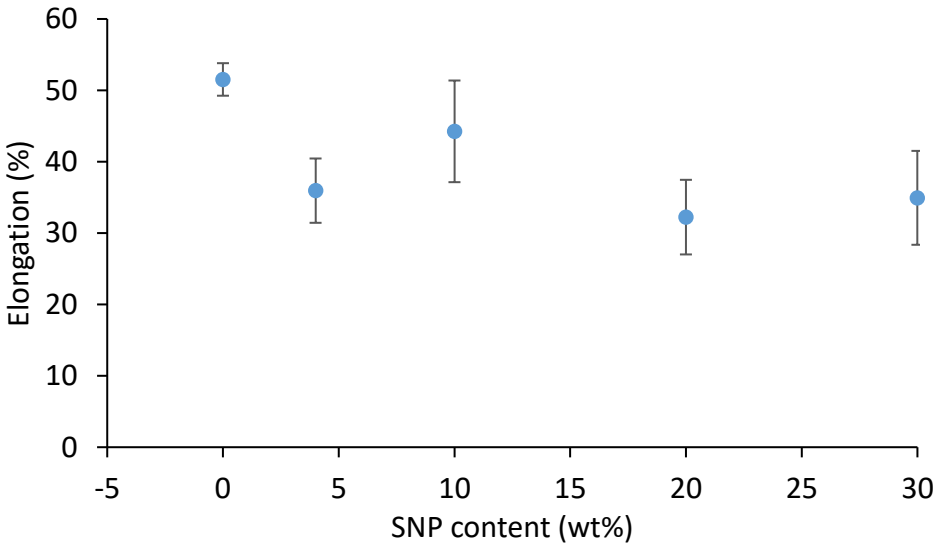

b)

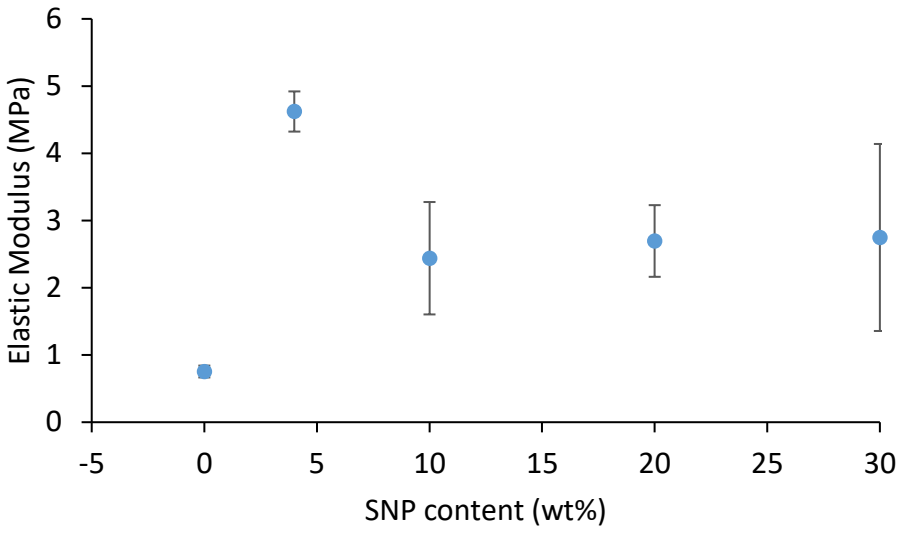

c)

Figure 2.19. The a) tensile strength, b) elongation and, c) elastic modulus of CS films reinforced with different amounts of SNPs.

As water is regarded as a plasticizer, films containing more water tend to be more ductile and flexible than the same films containing less water. **Fig. 2.20** shows the relationship between water content and SNP content for the SNP/HBCS and SNP/CS films. The films were subjected to moisture analyzer which is a closed balance with a heating function. The films were dried at 105 ^{o}C until their weight stayed constant. The moisture content of the films was determined by subtracting its initial weight to its final weight, then divided by its initial weight. Less water was retained in the films as the SNP content increased. Ma et al reported that the addition of SNPs created a tortuous path for water to pass through so that the water vapor permeability decreased.[36] The compactness of the films increased.[38] As a result, the SNP/HBCS films with higher SNP content were tougher (higher tensile strength) and less ductile (lower elongation) as SNP content increased compared to the SNP/CS films. The GY content did not affect the water content (grey and light blue circles in **Fig. 2.20**). As expected, lower water content was detected in the more hydrophobic SNP/HBCS films compared with the CS films (dark blue and light blue circles in **Fig.**

2.20). Not surprisingly, storing the films in a higher RH environment yielded films with higher moisture content (grey and orange circles in **Fig. 2.20**).

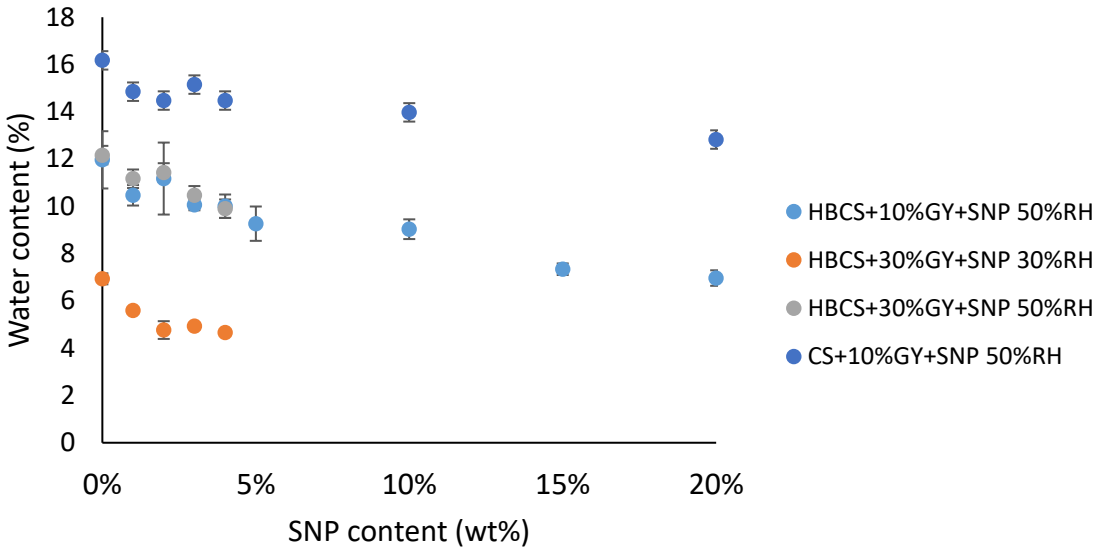

Figure 2.20. Water content of HBCS or CS films as a function of SNP content, GY, and humidity level.

2.4.2 Thermoresponsivity Evaluation of HBCS Dispersions using DSC and HBCS Films via Water Contact Angle Measurement

Before examining HBCS films or SNP/HBCS films for thermoresponsivity using DSC, aqueous dispersions of HBCS (MS = 1.8, LCST = 33 ºC as determined by light transmittance), ranging from 1 to 20 wt. %, were evaluated for thermoresponsivity using DSC. No obvious endothermic peak appeared (**Fig 2.21**). We began to suspect that perhaps DSC was not the best technique for determining the thermoresponsivity of our films. Therefore, we began to consider other approaches for determining the LCSTs of our films.

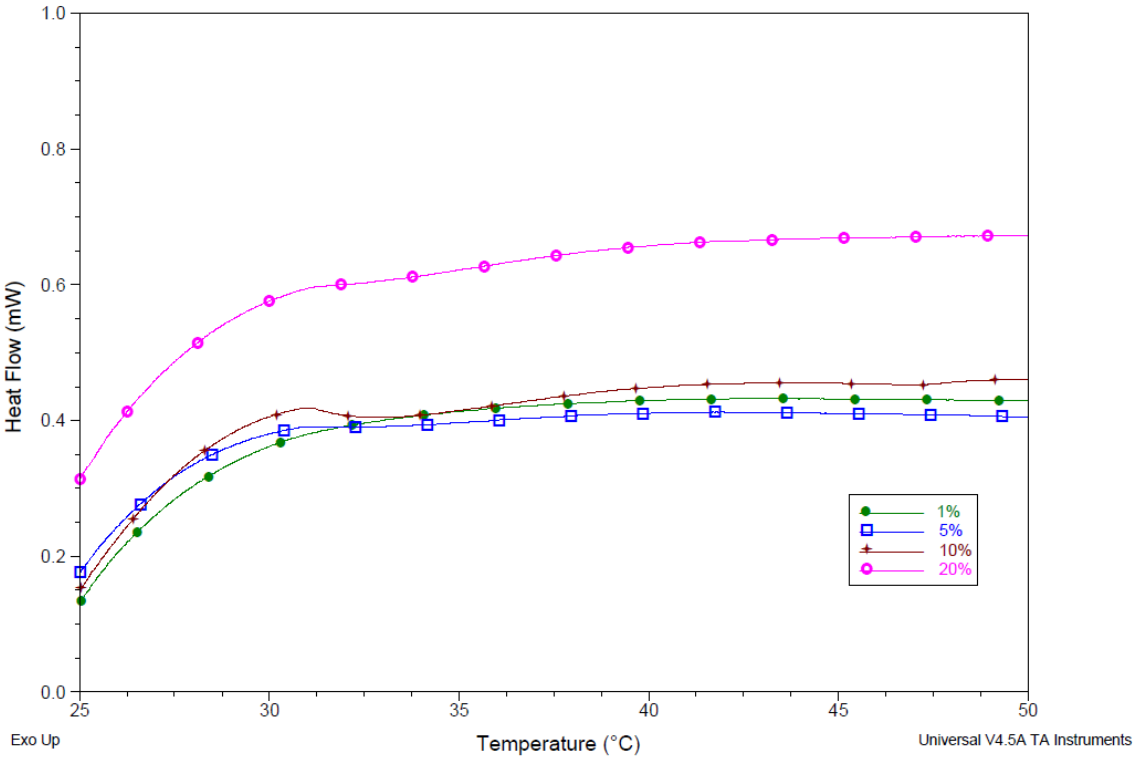

Figure 2.21. DSC thermogram of HBCS (MS = 1.8) aqueous dispersions of different concentrations.

Another approach that has been used to determine the thermoresponsivity of a film is by measuring the water contact angle as a function of temperature.[2] The contact angle is dependent upon the surface hydrophilicity of the film. Basically, how the water droplet interacts with the polymer surface is visually analyzed. The contact angle is regarded as the angle between the solid-liquid phase and liquid-gas phase (**Fig. 2.22)**. The material is considered hydrophobic if the angle is over 90 degrees or hydrophilic if it is lower than 90 degrees.[39]

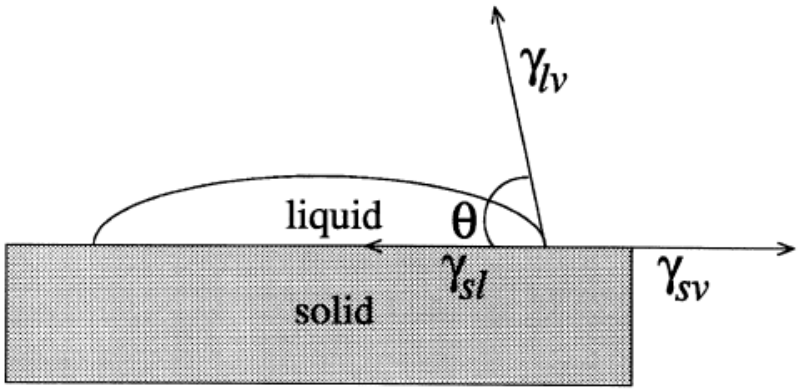

Figure 2.22. Scheme of a sessile-drop contact angle system. The contact angle is regarded as Θ. It is determined from Young's equation: $\gamma_{sv}-\gamma_{sl}-\gamma_{lv}COS\Theta = 0$, where γ_{sv}, γ_{sl} and γ_{lv} are defined as the interfacial tension between solid and vapor, solid and liquid, liquid and vapor.

Contact angle measurements were initially done on an HBCS film (MS = 1.83 LCST=33 ^{o}C) prepared using 10 wt. % GY at room temperature (25 ^{o}C). Glass was used as a comparison substrate. It was observed that the droplet on the HBCS film initially spread quickly and the contact angle decreased rapidly over the first 30 s, after which the contact angle decreased much more slowly and the droplet penetrated the film slowly which could not penetrate the glass (**Figs. 2.24, 2.25** and **2.26**). The volume of the droplet decreased in a linear fashion over time (**Fig. 2.26**). It is assumed that the volume loss of the droplet on glass is due to evaporation. In addition to evaporation, the HBCS film probably suffered from absorption resulting in a higher volume loss rate compared to glass.

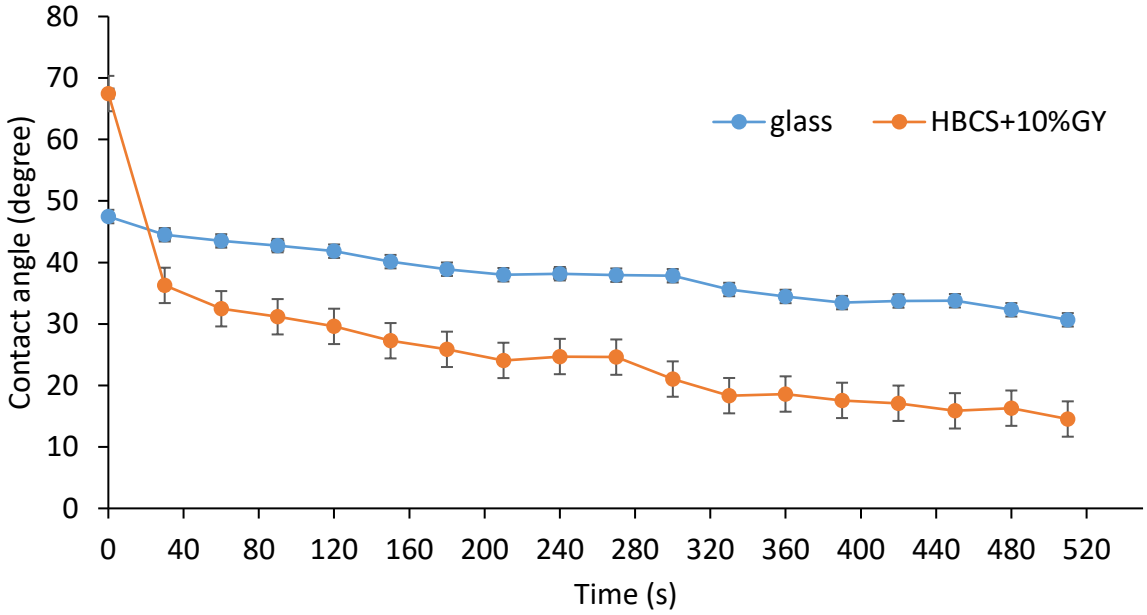

Figure 2.23.The contact angle of water on glass and HBCS films (10%GY) as a function of time.

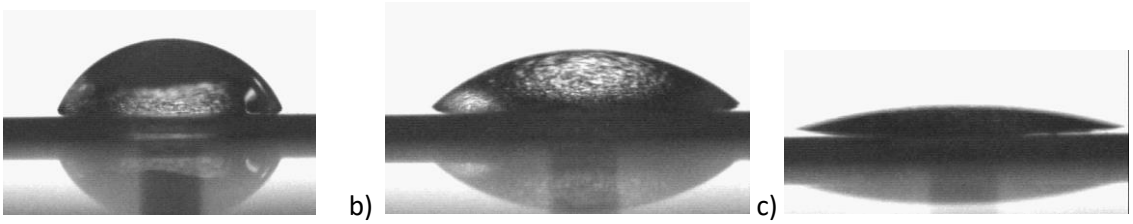

Figure 2.24. Pictures of water droplets on HBCS films (10%GY) at a) 0 s, b) 15 s and, c) 500s.

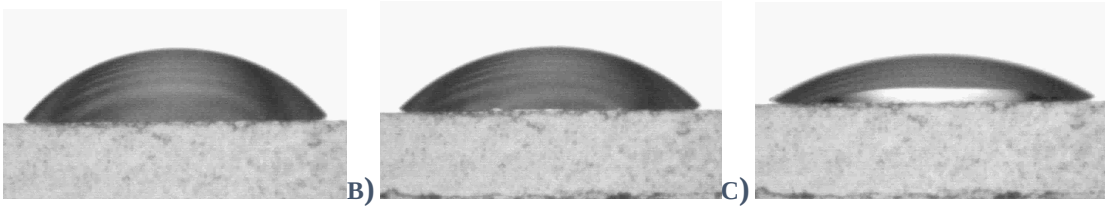

Figure 2.25. Pictures of water droplets on glass at a) 0 s, b) 15 s and, c) 500s.

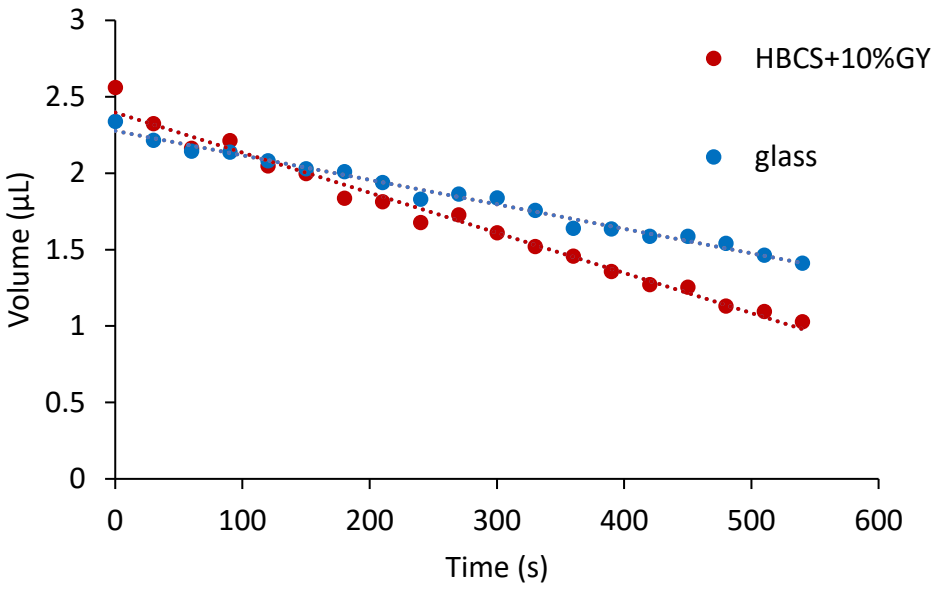

Figure 2.26. The volume of water droplets on glass and HBCS films (10 wt. %GY). The data was provided by video contact angle (VCA) analysis software.

The thermodynamic equilibrium between the three phrases should satisfy the Young's equation: $\gamma_{sv}-\gamma_{sl}-\gamma_{lv}COS\Theta = 0$, where γ_{sv}, γ_{sl}, γ_{lv} mean the interfacial tension between solid phase and vapor phase, solid phase and liquid phase, liquid phase and vapor phase (**Fig 2.20**), respectively. One of the basic assumptions is that the value of γ_{sv}, γ_{lv} and γ_{sl} are constant during the experiment. However, in our case, the water droplet slowly dissolved the HBCS films, which in turn altered γsl and γlv.[39] It may be possible to avoid dissolution by crosslinking the starch.

Another challenge is to provide a testing chamber with constant humidity at different temperatures so that the water evaporation rate would remain constant. As is shown in **Fig 2.25**, the water contact angle decreased much faster at 37 ^{o}C than at 25 ^{o}C due to faster water evaporation at 37 ^{o}C.

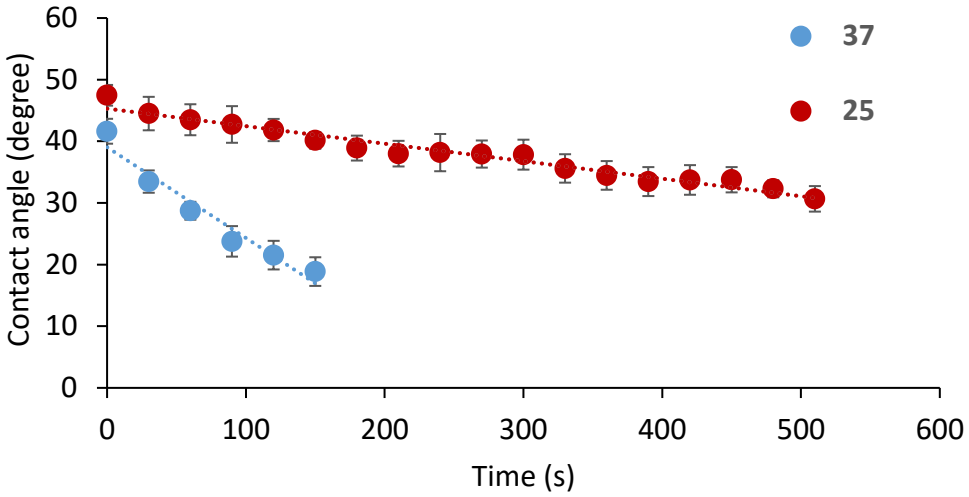

Figure 2.27. The contact angle of water on glass at 25 ºC and 37 ºC .

Chapter 3 Crosslinked Hydroxybutylated SNPs and Hydroxybutylated Corn Starch

3.1 Crosslinking Starch with Diisocyanates

As mentioned in **Section 2.4.2**, crosslinking the HBSNPs or HBCS is one possible strategy to increase the stability of the films in water and thus minimize the water penetration during the contact angle measurements.

Diisocyanates have been used to crosslink starch. This crosslinker generates essentially irreversible carbamate crosslinks between and within the polysaccharide chains. Barikani et al prepared urethane prepolymer crosslinked starch. (**Fig 3.1**) A prepolymer was prepared first by reacting polycaprolactone diol with hexamethylene diisocyanate (HMDI), generating a prepolymer with two free isocyanate groups at the ends. The hydrophobicity of the polymer increased with the addition of the prepolymer crosslinker compared with pure starch as determined via water contact angle measurements.[40]

Similar studies were also done by Tai et al who prepared starch-polyurethane films using HMDI modified PEG as the crosslinker.[41] The HMDI modified PEG was reacted with a gelatinized starch dispersion. The reaction mixture was cast and yielded a film in the Teflon mould. They reported that the surface hydrophobicity increased for the crosslinked starch films with respect to higher water contact angle. The crosslinked films started to display elastomeric behaviour with 10% crosslinker while bare starch films were brittle via tensile testing.[41]

3.2 HBSNPs Crosslinked with Hexamethylene Diisocyanate

We began the crosslinking studies using just HDMI as the crosslinker. HBSNPs (MS=1.31 LCST=49.5 ^{o}C) were crosslinked with HMDI using a procedure similar to that reported by

Barikani et al for cross-linking starch. Thus, HBSNPs (MS = 1.31, LCST = 49.5 ^{o}C) were dried in a vacuum oven overnight at 40 ^{o}C. They were dispersed in pyridine (10 wt. %). Then various amounts of HMDI (0.05 eq., 0.1 eq., or 0.25 eq. HMDI compared to anhydroglucose units) were added into the dispersion and the mixture stirred for 2 h at 65 ^{o}C (**Scheme 3.1**). During the reaction the mixture turned into a gel suggesting that crosslinking had occurred. The product was washed with methanol, filtered, dialysed and freeze-dried.

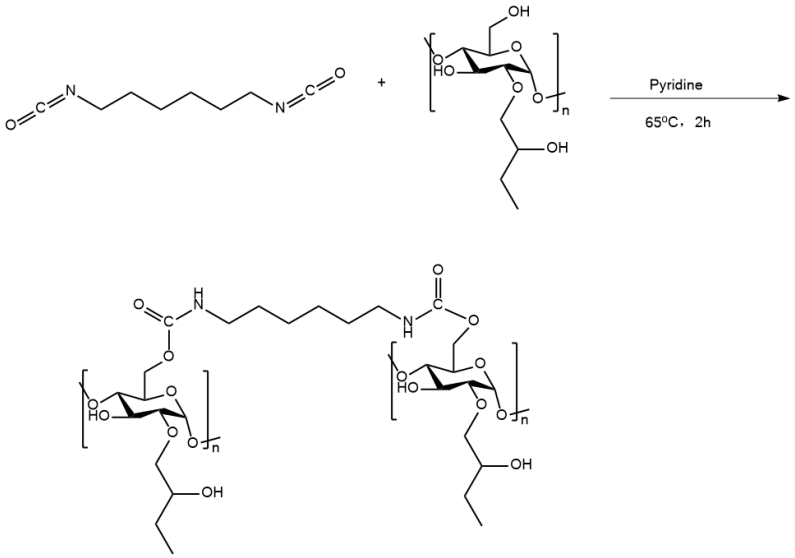

Scheme 3.1 The reaction of hexamethylene diisocynate (HMDI) with HBSNPs.

To further confirm the presence of the crosslink, IR spectra of the lyophilized material were obtained (**Fig. 3.2**). The appearance of an absorption at 1525 cm^{-1} was attributed to N-H bonding stretching of the newly formed carbamate group and the absorption at 1730 cm^{-1} was attributed to the C=O bond stretch of the carbamate group.

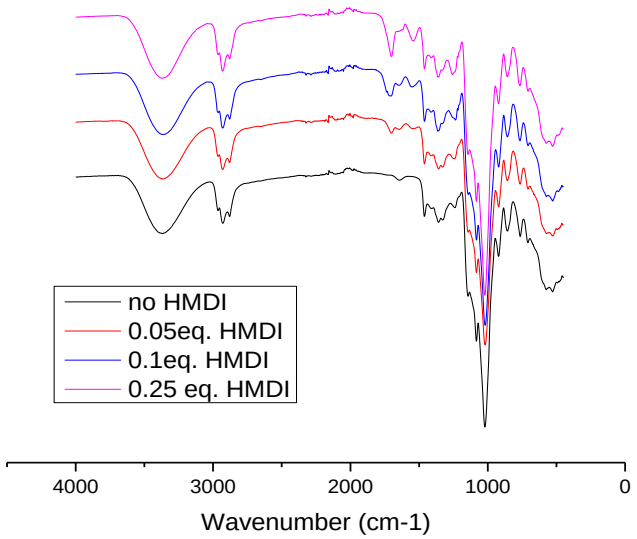

Figure 3.1. IR spectra of uncrosslinked HBNSPs and HMDI-crosslinked HBSNPs.

When gently heated with a heat gun, the gels appeared to undergo a phase transition as shown in **Fig. 3.3** for the HBSNPs crosslinked using 0.1 eq. HMDI. This suggested that the gels were thermoresponsive.

a)  b) 

Figure 3.2. Pictures of HBSNPs crosslinked using 0.1 eq. HMDI at a) ambient temperature; b) gentle heating with a heat gun.

The thermoresponsivity of the crosslinked HBSNPs was investigated using DSC. The crosslinked HBSNPs (20 mg in 1 mL DW) were allowed to fully swell overnight in water. The

mixture was centrifuged and the supernatant was discarded. The remaining gel was used for the DSC analysis. Strong endothermic peaks were evident in the thermogram indicating shrinkage or a phase transition of the gel (**Figs. 3.4** and **3.5**). This was not seen with the uncrosslinked HBSNPs (see **Section 2.2.2**) This could be attributed to the larger molecular weight of the crosslinked HBSNPs compared to uncrosslinked HBSNPs. Thus, when the gels shrink, they require more heat. Cong et al found that with the increasing chain length of pNIPAAM on pNIPAAM-PVP block copolymers, the endothermic peak intensity increased.[42] The peaks were broad compared with sharp peaks for pNIPAAM. Deng reported that crosslinked pNIPAAM microspheres showed shallower phase transitions with higher crosslinking densities as determined by measuring their hydrodynamic diameter as a function of temperature.[43] The temperature at the of lowest point in the thermogram is regarded to be the LCST of the sample. However, these results were not reproducible. For example, for the crosslinked HBSNPs that were prepared using 0.05 eq. HMDI (**Fig. 3.5**), the LCSTs varied from 46 ^{o}C to 66 ^{o}C. This was most certainly due to uneven x-linking of the HBSNPs which resulted in different crosslink densities within the gel.

The swelling ability of the gels was determined by water absorption. It was calculated as W_t-W_d/W_t, where W_t is the weight of the fully swollen gel and W_d is the weight of the gel after drying. The water absorption varied from 1.2 to 3 for the HBSNPs crosslinked with 0.05 eq. HMDI, which indicated the possibility of differential crosslink densities in the gels.

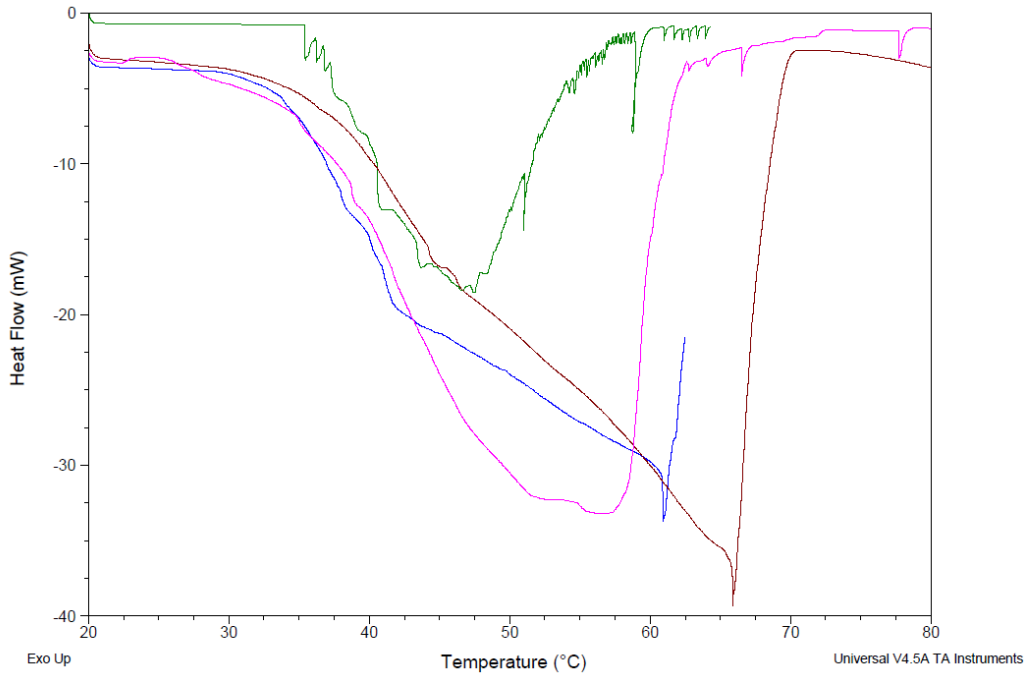

Figure 3.3. DSC thermogram of HBSNPs crosslinked using 0.05 eq. HMDI.

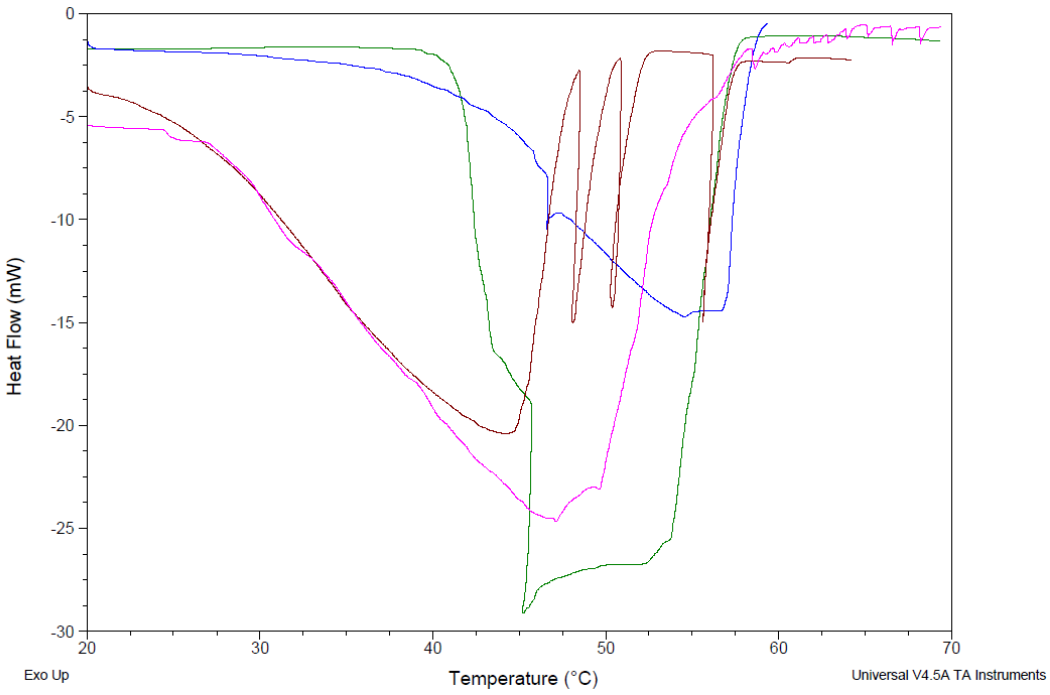

Figure 3.4. DSC thermogram of HBSNPs crosslinked using 0.1 eq. HMDI

Although the above crosslinking studies appeared to provide thermoresponsive gels and not films, we anticipated that reduced amount of crosslinker might generate crosslinked HBSNPs that would not gel and we would be able to cast thermoresponsive films. Therefore, we prepared HDMI cross-linked HBSNPs using only 0.03 eq., 0.01 eq., and 0.005 eq. of HMDI in dry DMSO as pyridine is more toxic. The reaction using 0.005 eq. of HMDI did not form gels during the reaction. The reaction mixtures were washed with methanol, dialyzed, cast on the silicone mould and air dried. Unfortunately, the films readily cracked.

3.3 Starch Films Prepared from HBCS Crosslinked with Oxidized Sucrose and Glyoxal

Recently, Xu et al prepared starch films using oxidized sucrose (OS) as a crosslinker. The OS was prepared by reacting sucrose with sodium periodate in distilled water at rt for 26 h (**Scheme 3.2**). Subsequently, barium chloride was added to precipitate excess salts. The mixture was filtered and the supernatant stored in the fridge as a 5 wt. % OS solution.[44]

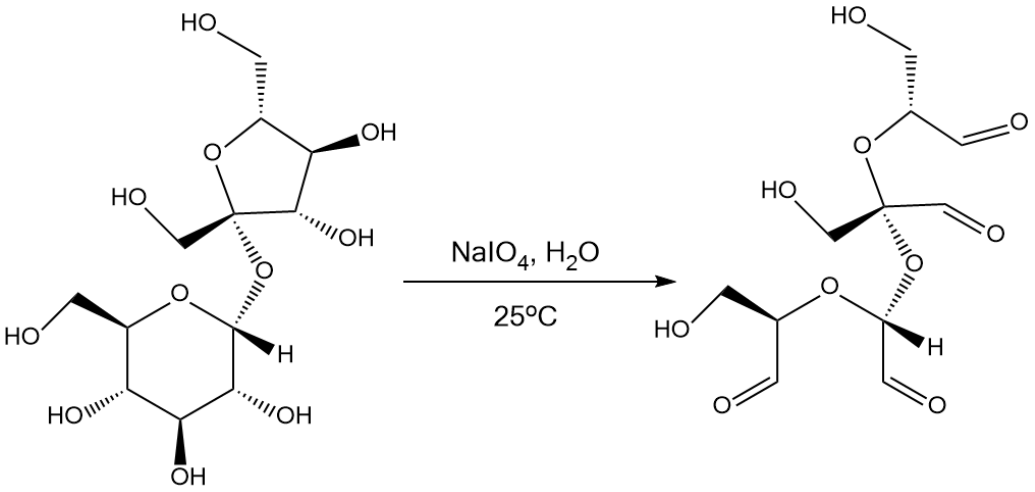

Scheme 3.2. Preparation of oxidized sucrose (OS).

Like other polyaldehyde crosslinkers, OS crosslinks starch by forming reversible acetal bonds with the hydroxy groups of the starch between and within the starch chains. Unlike other

polyaldehyde crosslinkers such as glutaraldehyde and formaldehyde, OS is bio-based and nontoxic. They reported that OS-crosslinked corn starch (CS) films were stable when stored in an environmental chamber (did not readily crack) and were stable in water retaining about 75% of their initial weight after being incubated in water for 35 days. In contrast, un-crosslinked ones retained only 20% of their initial weight over 30 days. It was found that films prepared with 15 wt. % of GY, crosslinked with 5 wt. % OS, and cured at 165 ^{o}C for 5 mins in the oven represented the optimum conditions to yield highest tensile strength and elongation. [44]

Before attempting to prepare HBSNP films crosslinked with OS, we attempted to reproduce Xu et al. results with CS. The OS solution was added to the dispersed starch mixture so that the final OS concentration equaled to 5 wt. % based on the weight of starch. The mixture was heated at 90 °C for 30 min. Subsequently, GY was added into the solution to make the final GY concentration equal to 15 wt. % based on the weight of starch and the resulting mixture was then poured onto a silicone substrate and air dried for 20 h. The film was further cured at 165 ^{o}C for 5mins, which was discribed as the optimum curing temperature and time.[44] The resulting film was conditioned in a humidity chamber (RH=60%) for 2 days before testing. The film was fairly stable in water in that it retained 70 wt. % of its weight (**Fig. 3.6**) after being soaked in water for 9 days. This result is somewhat similar to those of Xu et al who reported 75% retention after 10 days. We also determined the water stability of a film that was prepared in the same manner but not cured. This film lost 50% of its water within 3 days. The curing procedure results in the evaporation of water from the film which promotes the crosslinking reaction.

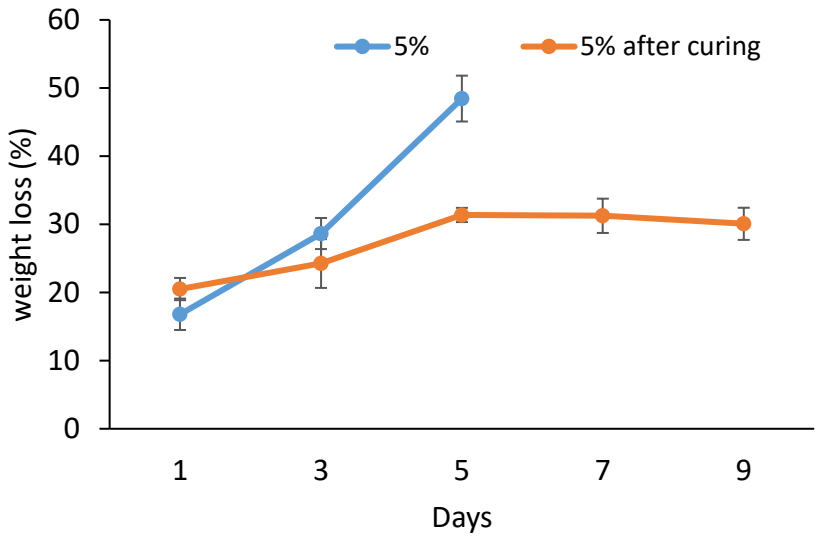

Figure 3.5. The weight loss of CS films crosslinked with 5% OS after being soaked in water for 1-9 days (the weight ratio of water to film was 25: 1). Blue line: not cured. Orange line: cured.

HBCS (MS = 1.83, LCST = 33 ^{o}C) films with 5 wt. % OS (0.02 eq per anyhydroglucose unit) were prepared with and without curing. Both of these films were unstable in water in that they both lost their integrity within hours when soaked in water. We noticed that, despite its hydrophobic appendage, the HBCS that was used to make the HBCS films was more water dispersible compared to the CS used to make the CS films. The HBCS was obtained by reacting CS with butene oxide at 40 ^{o}C for 24 h at pH 13. It is possible that, under these basic conditions, the CS degraded slightly during the synthesis of the HBCS. This possibly resulted in the HBCS having shorter polysaccharide chains compared to CS, which resulted in the HBCS being more dispersible than CS. It is possible that the longer chains of the CS results in OS-crosslinked CS films that were more stable in water than the OS-crosslinked HBCS films.

We reasoned that the water stability of the HBCS OS-crosslinked films could be increased by increasing the amount of OS (increasing the number of crosslinks). OS-crosslinked HBCS films were prepared using 0.25 eq., 0.5 eq. and 0.75 eq. of OS. The water stability of these films

did indeed increase with increasing OS; however, they were still quite unstable in that even when 0.75 eq. of was used, the resulting films exhibited 50% weight loss after incubation in water after 24 h (**Fig. 3.7**). Unfortunately, higher concentrations of OS resulted in the formation of gels.

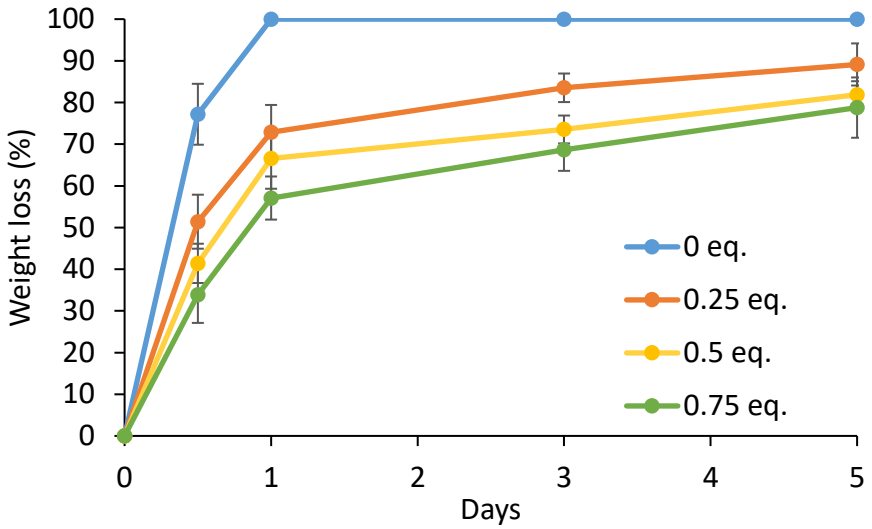

Figure 3.6. The weight loss of HBCS films crosslinked with varying amounts of OS after being soaked in water for 5 days (the weight ratio of water to film was 25:1).

To determine if a simpler reversible crosslinker would also impart greater water stability to HBCS films, HBCS films were prepared using 0.25 and 0.5 eq. of glyoxal (GX) as crosslinker (greater amounts of GX resulted in the formation of gels). The water stability of these films also increased with increasing GX; however, they too were still quite unstable in that even when 0.5 eq. of GX was used, the resulting films exhibited 50% weight loss after incubation in water after 24 h (**Fig. 3.8**).

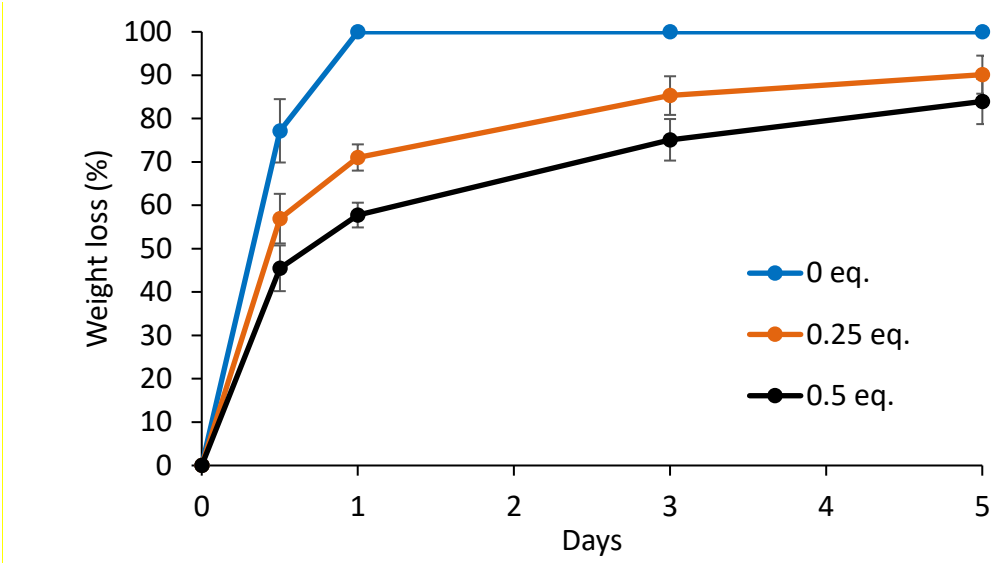

Figure 3.7. The weight loss of HBCS films crosslinked with 0.25 eq. and 0.5 eq. of GX after being soaked in water for 5 days (the weight ratio of water to film was 25:1).

The contact angle of the HBCS films prepared using 0.25 eq. and 0.5 eq. of GX was determined as a function of time (**Fig 3.9**). The crosslinked HBCS films had higher initial contact angles and a slower rate of decrease in the contact angle over the first 50 seconds compared to the uncrosslinked HBCS film.

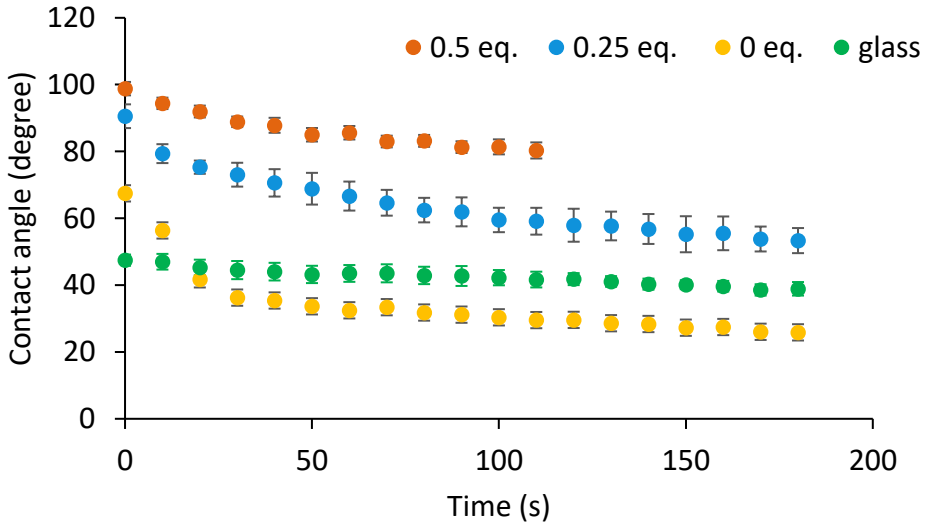

Figure 3.8. Contact angles of uncrosslinked and GX-crosslinked (0.25 or 0.5 eq.) HBCS films, and glass at rt.

How the water droplet volume changed with time was also studied. If the HBCS was indeed crosslinked, it was expected that water would penetrate more slowly into the film compared to the analogous uncrosslinked film. The rate of volume decrease of the water droplet on the 0.5 eq. GX-crosslinked HBCS film over 2 min was slightly slower compared to the uncrosslinked film or the 0.25 eq. GX-crosslinked HBCS film and was close to that of glass over 2 min (**Fig. 3.10**)(**Table 3.1**). This indicated that water penetration on the 0.5 eq. GX-crosslinked HBCS film was probably minimal over this time and that crosslinking appeared to have helped stabilize the HBCS films regarding water penetration. Contact angle and volume droplet measurements on the OS-crosslinked HBCS films are in progress.

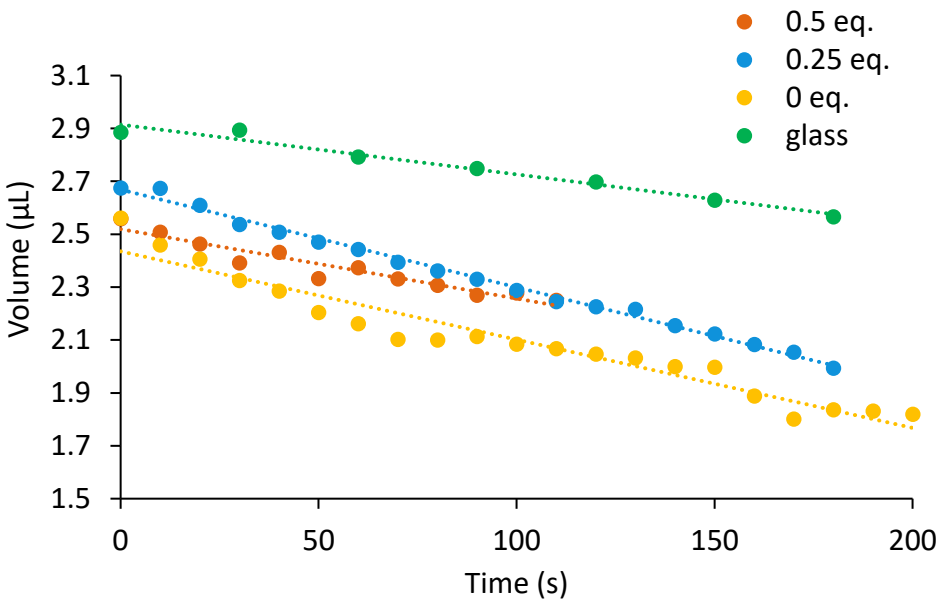

Figure 3.9. The water droplet volume on glass and uncrosslinked and GX-crosslinked HBCS films.

Table 3.1. The volume loss rate of water droplets on glass, uncrosslinked and GX-crosslinked HBCS films.

	Glass	**0 eq.**	**0.25 eq.**	**0.5 eq.**
dV/dt	-0.0019	-0.0033	-0.0037	-0.0026

Chapter 4 Summary and Future Work

4.1 Summary

In Chapter 2 we showed that films prepared from HBSNPs and using GY as plasticizer lacked stability in that they tended to readily crack and become brittle even when stored in a controlled humidity environment. We attempted to improve their stability using a variety of tactics. One was by using sorbitol or mixtures of sorbitol and GY as plasticizers but this was unsuccessful as these films readily cracked and were opaque. Blending the films with different amounts of PVA and GY generally did not produce stable films unless the amount of GY and PVA was very high (40 wt.% compared to the SNPs). The mechanical properties of the more stable HBSNP/PVA/GY films were determined by DMTA. Under 50 % RH, films with higher PVA had greater tensile strength and could be extended longer. We were unable to detect any thermal transitons of these films by DSC. Indeed, unlike pNIPAAM, whose thermal transition was readily detected by DSC, the thermal transition of the HBSNPs themselves was not readily detected by DSC. In any case, since these films required large amounts of PVA for stability and did not appear to be thermoresponsive (at least by DSC), we decided to pursue other approaches.

We attempted to prepare stable, thermoresponsive HBSNP films using PEG-grafted HBSNPs. However, the PEG-grafted HBSNPs were not readily dispersible, the yields of the PEG-grafted HBSNPs were low and the products were difficult to purify. Consequently, this approach was abandoned.

We then turned our attention to HBCS films reinforced with SNPs. The presence of SNPs appeared to enhance the physical properties of the HBCS films. However, we were unable to detect any thermal transitions of the HBCS itself by DSC (as was the case with the HBSNPs) which suggested to us that perhaps DSC is not the best method for determing the thermoresponsivity of our films. Since determining water contact angles as a function of

temperature has been used by others to determine the thermoresponsivity of films, we attempted to do this with the HBCS films. However, the HBCS films were not stable to water. It was concluded that crosslinking of the HBCS films would be necessary to provide the needed water stability for contact angle measurements.

In Chapter 3, we presented out attempts to produce air- and water-stable, crosslinked TR HBCS films. When using HMDI as a crosslinker (which forms an irreversible crosslink), we obtained either gels (at "high" HMDI) or films which readily cracked (at "low" HMDI). The gels appeared to be thermoresponsive as determined by DSC; however, we were unable to obtain accurate LCSTs for these gels as the results were difficult to reproduce, possibly due to different crosslink densities within the gel.

HBCS films crosslinked with GX or OS (which form reversible crosslinks) were also prepared. Although the GX and OS crosslinks appeared to increase the stability of the HBCS films in water, they were still not highly stable.

4.2 Future Work

Although we were unable to obtain air- (nonbrittle) and water-stable thermoresponsive starch films, we believe that such films can be obtained using crosslinked HBCS. Using HMDI as an irreversible crosslinker, we were able to obtain HBCS films (at low HMDI), but they were brittle. Using higher concentrations of HMDI, we obtained gels which appeared to be thermoresponsive by DSC. We anticipate that we can obtain stable TR films by: (a) using small amounts of a longer, more flexible diisocyanate crosslinker (such as a diisocyanate polyurethane prepolymer); (b) adding a solution of this crosslinker in DMSO (not neat as we did in Chapter 3) slowly to a dispersion of HBCS in DMSO (less toxic than pyridine) with vigorous stirring to ensure even crosslinking; (c) isolating the crosslinked HBCS (by precipitation in a different solvent) prior

to casting; and (4) dispersing the crosslinked HBCS in water in the presence of GY and then casting onto a substrate. These studies are in progress in the Taylor group.

Chapter 5 Experimental Procedure

5.1 General Information

Experimental SNPs were obtained from EcoSynthetix Inc. (Burlington, ON). Other reagents and solvents were commercially available and used without further purification unless stated otherwise. ^{1}H-NMR spectra were obtained on a Bruker Avance 500 MHz NMR spectrometer (Massachusetts, USA). Spectra obtained in D_2O were referenced to the HDO peak at 4.8 ppm. Spectra obtained in DMSO-d_6 were referenced to the solvent residual peaks at 2.5 ppm. Turbidity measurements were performed using a Cary 4000 Bio UV-Visible spectrophotometer from Agilent Technology Inc. (California, USA). Tensile testing was performed on a DMTA-V from Rheometric Scientific Inc (New Jersey, USA). Thermoresponsivity studies were done on a Q2000 Differential Scanning Calorimeter from TA instruments Inc. (Utah, USA). Water contact angle measurements were obtained using a Video Contact Angle System from AST Products Inc., (Massachusetts, USA). IR spectra were obtained using a Bruker Tensor IR spectrometer (Massachusetts, USA). Weight loss measurements were performed using a OHAUS Moisture Analyzer (New jersey, USA). Mass spectra of mPEG and mPEG-COOH were obtained from a Bruker Autoflex Speed MALDI mass spectrometer (Massachusetts, USA). Dithranol was used as the matrix. Sodium trifluoroacetate was used as the cationizing agent.

5.2 General Hydroxybutylation Protocol

SNPs (1 g) were dispersed in 2.7 mL deionized water in a 20 mL scintillation vial at 40 ^{o}C for 2 h. Upon cooling to rt, 0.3 mL of 10 M NaOH was added dropwise under vigorous stirring to give a dispersion with a pH 13. 1,2-butene oxide was added at rt. The vial was immediately put into a 40 ^{o}C water bath and the reaction mixture was vigorously stirred for 24 h. After 24 h, the

reaction mixture was cooled to rt and quenched with 1 M HCl under vigorous stirring. The neutralized reaction mixture was then subjected to dialysis against DW (1:100, v/v) for 1 to 2 days using a dialysis bag with molecular weight cut-off of 1 kD. A minimum of 5 water replacements were performed. The dialyzed SNPs were lyophilized to give a white powder. The white powder was stored in a centrifuge tube at rt.

For large-scale production, the reaction was conducted with mechanical stirring in a large round bottom flask. After quenching with aq. HCl, a five-fold excess (v/v) of isopropyl alcohol was added with vigorous stirring. This was then added to an acetone/isopropyl alcohol mixture (v/v,1:4) with vigorous mechanical stirring (volume ratio was 1:5) which resulted in the precipitation of the HBSNPs. The product was washed with acetone then air dried overnight. This precipitation protocol is only applicable to HBSNPs with low MS (around 1.3 or lower). HBSNPs with higher MS still required dialysis and freeze-drying for purification. For HBCS preparation, the procedure was the same except that 5 mL of DW per gram of CS was required to disperse well.

5.3 Light Transmittance Measurements

Light transmittance measurements were obtained using 1 wt. % aq. dispersions of the polymers unless stated otherwise. The samples were stirred in DW at 4 ^{o}C overnight and light transmittance was determined using a spectrophotometer equipped with a temperature controller. The temperature of the dispersion was measured by a temperature probe in a reference cell. The transmittance was recorded at 500 nm with a heating/cooling rate of 1 ^{o}C/min.

The dispersions were equilibrated for 2 minutes at an initial temperature in the cuvette before the measurements began. The data points were taken every 0.25 ^{o}C and recorded up to 70

^{o}C. The cloud point is defined as the temperature corresponding to the point which has the maximum derivative of the transmittance curve.

5.4 General Film Casting Protocol

5 wt. % HBSNP or HBCS dispersions were prepared first, followed by the addition of a certain amount of plasticizer and the mixture was stirred overnight. The mixture was cast on a silicone mould or a silicone sheet on a leveled surface in the fume hood. Once dried, the films were stored in the environmental chamber under desired humidity. The environmental chamber was a desiccator containing a saturated salt solution. Different saturated salt solutions can provide different humidity levels. Here saturated solutions of potassium acetate (15% RH), potassium carbonate (50% RH) and sodium bromide (60% RH) were used. The RH was monitored using a humidity meter.

5.5 Procedures for mPEG-COOH Preparation and mPEG grafted HBSNPs Reactions

(a) Preparation of mPEG-grafted HBSNPs using succinic acid as linker

4 g of mPEG (Mn 2000) and 0.4 g of succinic anhydride (2 eq.) in 50 mL toluene in a three-neck flask equipped with a Dean Stark apparatus was heated to reflux for 2 h. As temperature increased, the mPEG melted. Subsequently, 1 g of HBSNPs (MS = 1.3, LCST = 50 ^{o}C) was added. The heterogenous mixture refluxed for another 2 hours. After cooling to rt, the mixture was filtered. The solids were dissolved in DW and dialyzed against DW for 2 days using a dialysis membrane with a 100 kD cut-off then freeze-dried to give a white powder.[32]

(b) mPEG-COOH

Chromic acid (1M) was prepared by adding 2 g of CrO_3 to 2.8 mL of DW, cooling to 0 ^oC, followed by the addition of 1.7 mL of 18 M sulfuric acid. The volume was adjusted to 20 mL by adding DW. mPEG (M_n 2000 g mol^{-1}, 500 mg) was dispersed in 10 mL acetone and 500 μL chromic acid (2 eq.) was added dropwise. After 5 hours, isopropyl alcohol was added to quench the reaction followed by the addition of DW. The solution was extracted with 20 mL dichloride methylene three times and further washed with saturated sodium chloride solution. The organic layer was dried (sodium sulfate), concentrated by rotary evaporation then precipitated in 20 mL ether to give mPEG-COOH as a white powder.[34]

HBSNPs and mPEG-COOH were dried in a vacuum oven at 40 ^oC overnight to remove moisture. HBSNPs (0.5 g, MS = 1.26, LCST = 50 ^oC) and a pre-determined amount of mPEG-COOH were dissolve in 7 mL of dry DMSO with addition of EDC (2.5 eq. to mPEG-COOH) and a catalytic amount of DMAP (0.1 eq. to mPEG-COOH) at rt. The reaction mixture was stirred at rt for 2 days and then dialyzed against DW using a dialysis membrane with a 100 kd cut-off for 5 days. The water was replaced 10 times. The reaction mixture was diluted to $1:10^{20}$. After dialysis the mixture was freeze-dried to yield a white powder.[35]

The reaction efficiency can be estimated from analysis of the NMR spectrum (See **Section 2.3.1, Fig 2.12**). The methylene protons on mPEG overlapped with the C-H protons (6 protons in the anhydroglucose unit and 3 protons in the HB group) on the HBSNPs (3.2 ppm-4.3 ppm). The integral of the C-H protons on HBSNPs(MS=1.26) was calculated as 6+1.26×3=9.78. From the NMR spectrum of mPEG-HBSNP using 0.05 eq. mPEG-COOH, the integral of the peaks from 3.2 ppm to 4.3 ppm was 16.6. So, the integral for the methylene protons on mPEG was 16.6-9.78=6.82. There were 176 methylene protons in a mPEG-COOH (M_n 2000). The reaction efficiency was calculated as 6.82×100%/176×0.05= 78%

5.6 Procedures for Crosslinking HBSNP or HBCS Reactions

a) Crosslinking HBSNPs with HMDI

1 g of HBSNPs (MS = 1.31, LCST = 49.5 ^{o}C) was dispersed in 10 mL pyridine in a 20 mL glass vial in a water bath set to 40 ^{o}C. The temperature of the water bath was elevated to 65 ^{o}C and then a pre-determined amount of HMDI was added (0.25 eq., 0.1 eq., 0.05eq.) with vigorous stirring. The reaction mixture turned into a gel within an hour. The gel was removed, macerated and then washed with methanol with vigorous stirring several times. The washed gels were subjected to vacuum filtration to remove the methanol. Water was added to the solid gels and the resulting suspension dialyzed against DW for 2 days using a dialysis bag with a 1 kD cut-off (5 times water replacement). After freeze drying, white powders were obtained. Reactions with lower amounts of HMDI were conducted exactly in the same way except in dry DMSO (1 g in 11 mL). The reaction with 0.005 eq. of HMDI gave a very viscous liquid reaction mixture instead of a gel and was subjected to dialysis directly.

b) Crosslinking HBCS with GY or OS

(a) Preparation of OS[6]

Sucrose (6.6 g) and sodium periodate (12.9 g) were dissolved in 200 mL of DW and stirred at rt for 26 h followed by the addition of 7 g barium chloride. The mixture was stirred for one hour at 5 ^{o}C to precipitate the salts. The mixture was filtered to give an OS solution (5 wt. %).[44]

(b) OS crosslinked films

In order to perform the crosslinking reaction in a concentrated solution, the OS solution was first concentrated down to 10 wt. % by rotary evaporation, which gave an orange-coloured solution. OS dispersions (10 wt. %) (0.25 eq., 0.5eq., 0.75 eq. of OS to HBCS) were added to a 10

wt. % HBCS (MS = 1.83, LCST = 33 ºC) aqueous dispersion followed by the addition of GY (15 wt. % to HBCS) then stirred at 4 ºC overnight. As we did not isolate the OS and characterize it, the molar mass of OS was determined, as Xu et al reported, to be 325.25 g/mol, which is the average value of the maximum weight (the weight of sucrose, 342.49 g/mol) and the minimum weight (the weight of oxidized sucrose with 4 aldehyde groups per molecule, 308.00 g/mol).[44] Formic acid (1 eq.) was added, stirring for another 3 hours at room temperature. Then solutions were cast on the silicone sheet and air-dried in the fume hood. The films were stored under 60% RH for further characterization.

For the crosslinked CS films, an OS dispersion (5wt.%) was diluted to disperse corn starch to make the final 5 wt. % OS concentration 5wt.% based on the weight of starch. The mixture was stirred at 90 ºC for 30 mins. Then, 15 wt.% GY based on the weight of starch was added and mixed well, then poured on the silicone substrate for air drying. Films were cured in the oven at 165 ºC for 5 mins and stored under 60% RH.

The crosslinking reactions involving GX are similar to OS crosslinking reactions. The GX solution was used at a concentration of 40 wt.%.

5.6 Tensile Testing

Films with a thickness of 100 μm to 300 μm as determined using calipers, were used. The films were cut into strips of 4 cm in length and 1cm in width. The thickness was calculated as the average value resulting from three times measurement of the strip. The thickness difference bertween the sample was between 10 % an 15 %. The samples were loaded between the grips and stretched at 0.05 %/s until they broke. Stress-strain curves were obtained where the tensile strength and elongation were known. From the initial elastic linear part of the curve, the elastic modulus was calculated.

5.7 DSC Measurements

For DSC measurements of crosslinked HBSNPs, samples were prepared by adding 20 mg of crosslinked HBSNPs to 1 mL of DW in an Eppendorf tube and then mixed on a rotatory mixer overnight. The mixture was centrifuged for 10 s and then the supernatant was decanted and the remaining gel was used for DSC measurements. For HBSNPs or HBCS, dispersions of different concentrations were prepared by mixing HBSNPs or HBCS in DW at 4 ^{o}C overnight.

In a typical DSC experiment, 10 mg of sample (gel or dispersions) was sealed in a hermetic aluminium pan using a hermetic lid. A similar same amount of DW was prepared in the same way for reference. Two pans were loaded on the sample holders and the pans were heated from 20 ^{o}C to 80 ^{o}C with heating rate of 2 ^{o}C/min under a dry nitrogen flow of 80 ml/min.

5.8 Water Contact Angle Measurements

Samples were cut into squares and fixed on the white plastic board on the platform of a video contact angle system using tapes. A 10 mL syringe containing DW was loaded in the instrument. With a 3 μL water drop attached to the needle, the platform was moved up until the water droplet detached from the needle and landed on the sample. The platform was then moved down slowly. How the water droplet transformed on the sample was recorded for 3 to 5 mins. Desired frames from the video were analyzed to calculate the water contact angle with an interval of 10 s unless stated otherwise using VCA optima software.

5.9 Stability Test in Water and Moisture Content Measurement

A film (W_i = 0.5 g) was immersed in water (25-fold excess by wt.) for different amounts of time. The remaining film was drained gently and dried using a moisture analyzer at 110 ^{o}C in

an aluminum pan until a constant weight was obtained which was the weight of remaining film (W_r). The weight loss was calculated as $(W_i - W_r) \times 100\%/W_i$

The moisture content of the films was also determined using a moisture analyzer by drying at 110 ^oC until a constant weight W_f was reached. The oisture content was calculated as $(W_i - W_f) \times 100\%/W_i$

Reference

(1) Boateng, J. S.; Matthews, K. H.; Stevens, H. N. E.; Eccleston, G. M. Wound Healing Dressings and Drug Delivery Systems: A Review. *J. Pharm. Sci.* **2008**, *97* (8), 2892–2923.

(2) Abdali, Z.; Yeganeh, H.; Solouk, A.; Gharibi, R.; Sorayya, M. Thermoresponsive Antimicrobial Wound Dressings via Simultaneous Thiol-Ene Polymerization and in Situ Generation of Silver Nanoparticles. *RSC Adv* **2015**, *5* (81), 66024–66036.

(3) Kevin, M. *Dynamic Mechanical Analysis: A Practical Introduction*, second edition.; CRC Press, **2008**.

(4) Radhakumary, C.; Antonty, M.; Sreenivasan, K. Drug Loaded Thermoresponsive and Cytocompatible Chitosan Based Hydrogel as a Potential Wound Dressing. *Carbohydr. Polym.* **2011**, *83* (2), 705–713.

(5) Klouda, L.; Mikos, A. G. Thermoresponsive Hydrogels in Biomedical Applications. *Interact. Polym. Pharm. Biomed. Appl.* **2008**, *68* (1), 34–45.

(6) Reddy, T. T.; Kano, A.; Maruyama, A.; Hadano, M.; Takahara, A. Thermosensitive Transparent Semi-Interpenetrating Polymer Networks for Wound Dressing and Cell Adhesion Control. *Biomacromolecules* **2008**, *9* (4), 1313–1321.

(7) Wu, C.; Wang, X. Globule-to-Coil Transition of a Single Homopolymer Chain in Solution. *Phys Rev Lett* **1998**, *80* (18), 4092–4094.

(8) Le Corre, D.; Bras, J.; Dufresne, A. Starch Nanoparticles: A Review. *Biomacromolecules* **2010**, *11* (5), 1139–1153.

(9) Jiménez, A.; Fabra, M. J.; Talens, P.; Chiralt, A. Edible and Biodegradable Starch Films: A Review. *Food Bioprocess Technol.* **2012**, *5* (6), 2058–2076.

(10) Kong, L.; Ziegler, G. R. Fabrication of Pure Starch Fibers by Electrospinning. *Food Hydrocoll.* **2014**, *36*, 20–25.

(11) Lee, K. Y.; Jeong, L.; Kang, Y. O.; Lee, S. J.; Park, W. H. Electrospinning of Polysaccharides for Regenerative Medicine. *Adv. Drug Deliv. Rev.* **2009**, *61* (12), 1020–1032.

(12) Rindlav-Westling, A.; Stading, M.; Hermansson, A.-M.; Gatenholm, P. Structure, Mechanical and Barrier Properties of Amylose and Amylopectin Films. *Carbohydr. Polym.* **1998**, *36* (2), 217–224.

(13) Rindlav-Westling, A.; Stading, M.; Gatenholm, P. Crystallinity and Morphology in Films of Starch, Amylose and Amylopectin Blends. *Biomacromolecules* **2002**, *3* (1), 84–91.

(14) Park, H. R.; Chough, S. H.; Yun, Y. H.; Yoon, S. D. Properties of Starch/PVA Blend Films Containing Citric Acid as Additive. *J. Polym. Environ.* **2005**, *13* (4), 375–382.

(15) Torres, F. G.; Commeaux, S.; Troncoso, O. P. Starch-Based Biomaterials for Wound-Dressing Applications. *Starch - Stärke* **2013**, *65* (7-8), 543–551.

(16) Zhou, L. H.; Nahm, W. K.; Badiavas, E.; Yufit, T.; Falanga, V. Slow Release Iodine Preparation and Wound Healing: In Vitro Effects Consistent with Lack of in Vivo Toxicity in Human Chronic Wounds. *Br. J. Dermatol.* **2002**, *146* (3), 365–374.

(17) Kota, S.; Adibhatla, K. S. B. R.; Venkaiah, C. N. *Improved Process for the Preparation of Cadexomer Iodine*; Google Patents, **2008**.

(18) Wittaya-areekul, S.; Prahsarn, C. Development and in Vitro Evaluation of Chitosan–polysaccharides Composite Wound Dressings. *Int. J. Pharm.* **2006**, *313* (1–2), 123–128.

(19) Pang, S. C.; Chin, S. F.; Tay, S. H.; Tchong, F. M. Starch–maleate–polyvinyl Alcohol Hydrogels with Controllable Swelling Behaviors. *Carbohydr. Polym.* **2011**, *84* (1), 424–429.

(20) Ju, B.; Yan, D.; Zhang, S. Micelles Self-Assembled from Thermoresponsive 2-Hydroxy-3-Butoxypropyl Starches for Drug Delivery. *Carbohydr. Polym.* **2012**, *87* (2), 1404–1409.

(21) Ju, B.; Cao, S.; Zhang, S. Effect of Additives on the Cloud Point Temperature of 2-Hydroxy-3-Isopropoxypropyl Starch Solutions. *J. Phys. Chem. B* **2013**, *117* (39), 11830–11835.

(22) Ju, B.; Zhang, C.; Zhang, S. Thermoresponsive Starch Derivates with Widely Tuned LCSTs by Introducing Short Oligo(ethylene Glycol) Spacers. *Carbohydr. Polym.* **2014**, *108*, 307–312.

(23) Yuan, X.; Ju, B.; Zhang, S. Novel pH- and Temperature-Responsive Polymer: Tertiary Amine Starch Ether. *Carbohydr. Polym.* **2014**, *114*, 530–536.

(24) Magda, K. M.Sc. Thesis. *Univ. Waterloo.* **2015**.

(25) Zheng, B. W. M.Sc. Thesis. *Univ. Waterloo.* **2016**.

(26) Krogars, K.; Heinämäki, J.; Karjalainen, M.; Niskanen, A.; Leskelä, M.; Yliruusi, J. Enhanced Stability of Rubbery Amylose-Rich Maize Starch Films Plasticized with a Combination of Sorbitol and Glycerol. *Int. J. Pharm.* **2003**, *251* (1–2), 205–208.

(27) Tang, X.; Alavi, S. Recent Advances in Starch, Polyvinyl Alcohol Based Polymer Blends, Nanocomposites and Their Biodegradability. *Carbohydr. Polym.* **2011**, *85* (1), 7–16.

(28) Luo, X.; Li, J.; Lin, X. Effect of Gelatinization and Additives on Morphology and Thermal Behavior of Corn starch/PVA Blend Films. *Carbohydr. Polym.* **2012**, *90* (4), 1595–1600.

(29) Tian, H.; Yan, J.; Rajulu, A. V.; Xiang, A.; Luo, X. Fabrication and Properties of Polyvinyl Alcohol/starch Blend Films: Effect of Composition and Humidity. *Int. J. Biol. Macromol.* **2017**, *96*, 518–523.

(30) Bartczak, Z.; Galeski, A. Mechanical Properties of Polymer Blends. In *Polymer Blends Handbook*; Utracki, L. A., Wilkie, C. A., Eds.; Springer Netherlands: Dordrecht, **2014**; pp 1203–1297.

(31) Movagharnezhad, N.; Moghadam, P. N. Synthesis of Methoxy Poly (ethylene Glycol)/starch Grafted Copolymers and Investigation of Their Drug Release Behavior. *Starch - Stärke 68* (3-4), 314–320.

(32) Wang, J.; Zhai, W.; Zheng, W. Poly(Ethylene Glycol) Grafted Starch Introducing a Novel Interphase in Poly(Lactic Acid)/Poly(Ethylene Glycol)/Starch Ternary Composites. *J. Polym. Environ.* **2012**, *20* (2), 528–539.

(33) Yang, Z.; Zhang, W.; Zou, J.; Shi, W. Synthesis and Thermally Responsive Characteristics of Dendritic Poly(ether-Amide) Grafting with PNIPAAm and PEG. *Polymer* **2007**, *48* (4), 931–938.

(34) Fishman, A.; Acton, A.; Lee-Ruff, E. A Simple Preparation of PEG-Carboxylates by Direct Oxidation. *Synth. Commun.* **2004**, *34* (12), 2309–2312.

(35) Zhang, A.; Zhang, Z.; Shi, F.; Ding, J.; Xiao, C.; Zhuang, X.; He, C.; Chen, L.; Chen, X. Disulfide Crosslinked PEGylated Starch Micelles as Efficient Intracellular Drug Delivery Platforms. *Soft Matter* **2013**, *9* (7), 2224–2233.

(36) Ma, X.; Jian, R.; Chang, P. R.; Yu, J. Fabrication and Characterization of Citric Acid-Modified Starch Nanoparticles/Plasticized-Starch Composites. *Biomacromolecules* **2008**, *9* (11), 3314–3320.

(37) Nunes, R. W.; Martin, J. R.; Johnson, J. F. Influence of Molecular Weight and Molecular Weight Distribution on Mechanical Properties of Polymers. *Polym. Eng. Sci.* **2004**, *22* (4), 205–228.

(38) Shi, A.; Wang, L.; Li, D.; Adhikari, B. Characterization of Starch Films Containing Starch Nanoparticles: Part 1: Physical and Mechanical Properties. *Carbohydr. Polym.* **2013**, *96* (2), 593–601.

(39) Kwok, D. Y.; Neumann, A. W. Contact Angle Measurement and Contact Angle Interpretation. *Adv. Colloid Interface Sci.* **1999**, *81* (3), 167–249.

(40) Barikani, M.; Mohammadi, M. Synthesis and Characterization of Starch-Modified Polyurethane. *Carbohydr. Polym.* **2007**, *68* (4), 773–780.

(41) Tai, N. L.; Adhikari, R.; Shanks, R.; Adhikari, B. Flexible Starch-Polyurethane Films: Physiochemical Characteristics and Hydrophobicity. *Carbohydr. Polym.* **2017**, *163*, 236–246.

(42) Cong, H.; Li, J.; Li, L.; Zheng, S. Thermoresponsive Gelation Behavior of poly(N-Isopropylacrylamide)-Block-poly(N-Vinylpyrrolidone)-Block-poly(N-Isopropylacrylamide) Triblock Copolymers. *Eur. Polym. J.* **2014**, *61*, 23–32.

(43) Deng, Y. H.; Wang, C. C.; Shen, X. Z.; Yang, W. L.; Jin, L; Gao, H; Fu, S. K. Preparation, Characterization, and Application of Multistimuli-Responsive Microspheres with Fluorescence-Labeled Magnetic Cores and Thermoresponsive Shells. *Chem. – Eur. J.* **2005**, *11* (20), 6006–6013.

(44) Xu, H.; Canisag, H.; Mu, B.; Yang, Y. Robust and Flexible Films from 100% Starch Cross-Linked by Biobased Disaccharide Derivative. *ACS Sustain. Chem. Eng.* **2015**, *3* (11), 2631–2639.

Appendix

Selected Stress-Strain Curves

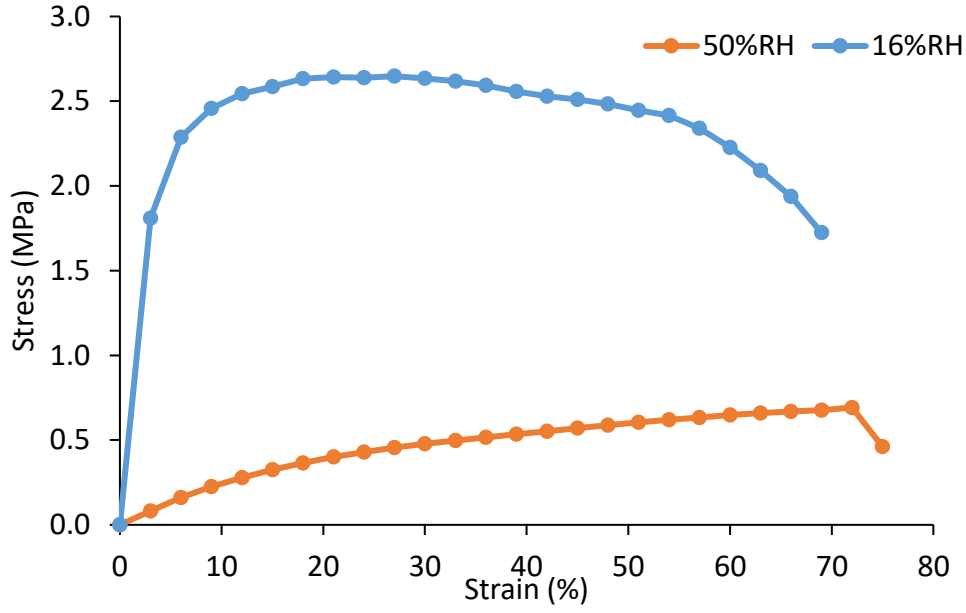

(a)

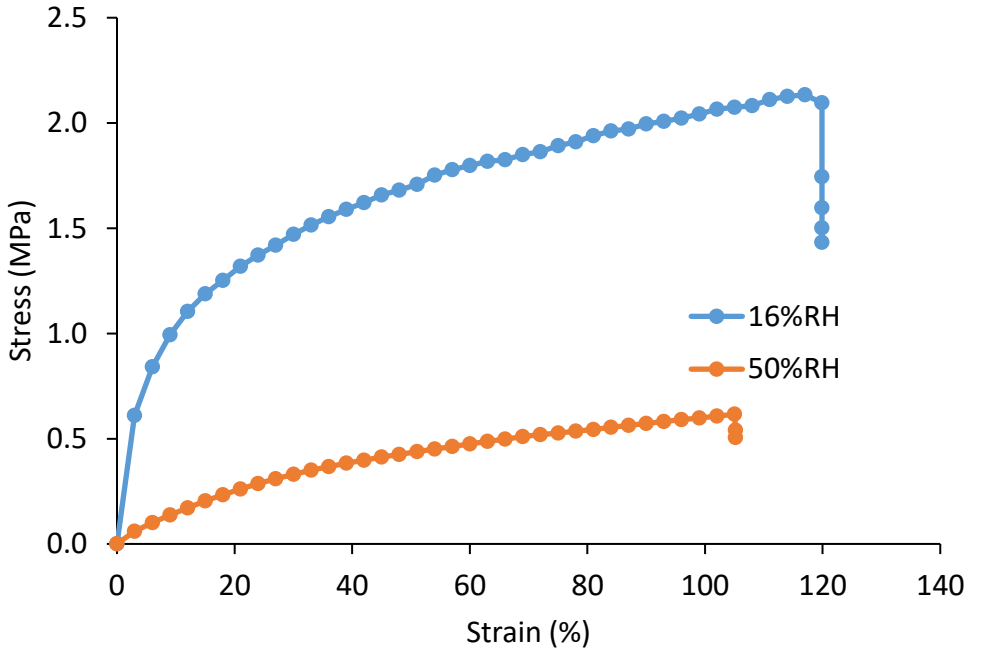

(b)

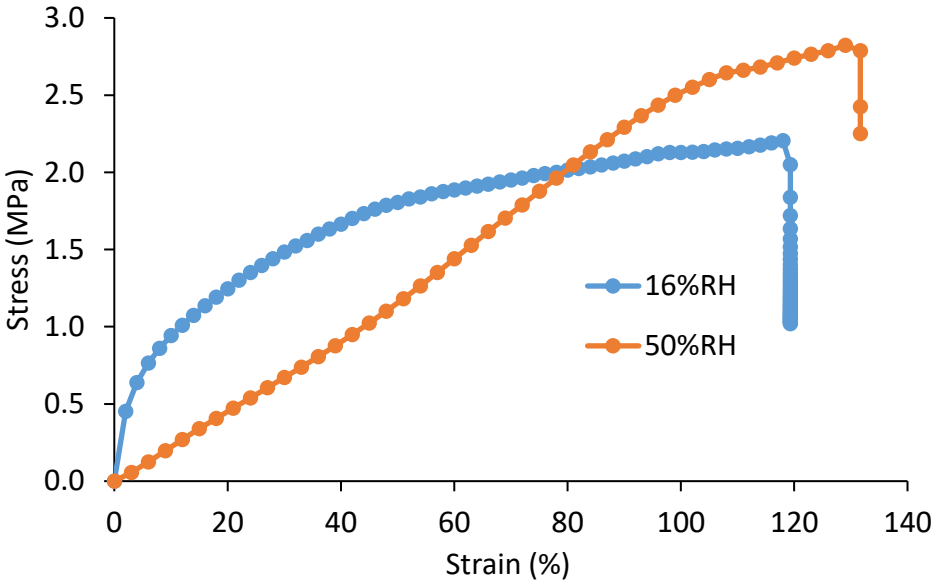

(c)

Figure A 2.2.1 Typical Stress-Strain curves of (a) HBSNP/PVA/GY films consisting of 56 % HBSNP, 22 % PVA and 22 % GY. (b) HBSNP/PVA/GY films consisting of 50 % HBSNP, 25 % PVA and 25 % GY (c) HBSNP/PVA/GY films consisting of 45% HBSNP, 27.5 % PVA and 27.5 % GY. All the films were stored under 16 % RH or 50 % RH for at least 2 days.